How to cite: *Angew. Chem. Int. Ed.* **2024**, *63*, e202306503
doi.org/10.1002/anie.202306503

CO_2 Electrolysis

Effects of Iron Species on Low Temperature CO_2 Electrolyzers

Anna F. Staerz, Marieke van Leeuwen, Tatiana Priamushko, Torben Saatkamp, Balázs Endrődi, Nina Plankensteiner, Matias Jobbagy, Sohrab Pahlavan, Martijn J. W. Blom, Csaba Janáky, Serhiy Cherevko, and Philippe M. Vereecken*

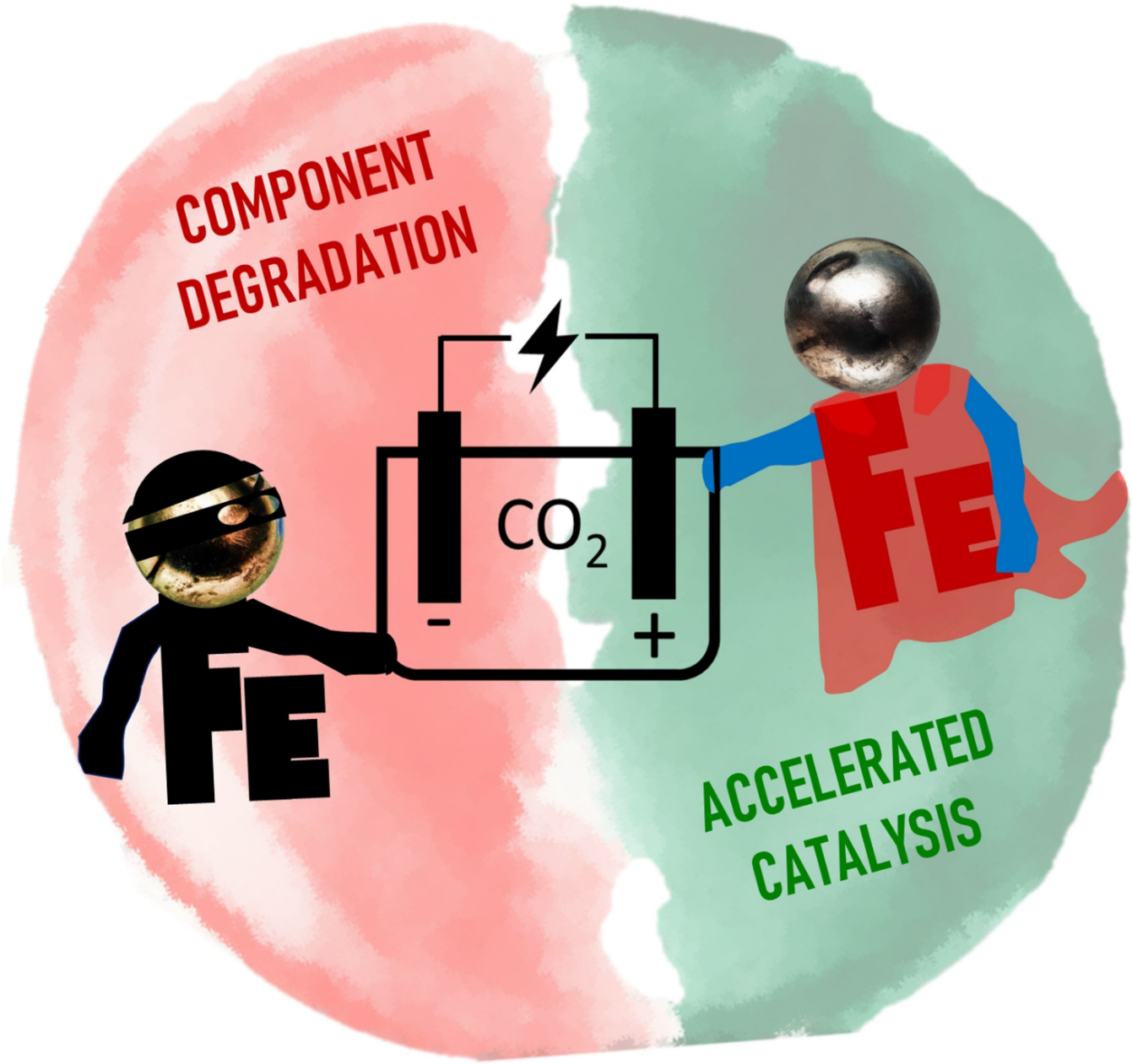

Abstract: Electrochemical energy conversion devices are considered key in reducing CO_2 emissions and significant efforts are being applied to accelerate device development. Unlike other technologies, low temperature electrolyzers have the ability to directly convert CO_2 into a range of value-added chemicals. To make them commercially viable, however, device efficiency and durability must be increased. Although their design is similar to more mature water electrolyzers and fuel cells, new cell concepts and components are needed. Due to the complexity of the system, singular component optimization is common. As a result, the component interplay is often overlooked. The influence of Fe-species clearly shows that the cell must be considered holistically during optimization, to avoid future issues due to component interference or cross-contamination. Fe-impurities are ubiquitous, and their influence on single components is well-researched. The activity of non-noble anodes has been increased through the deliberate addition of iron. At the same time, however, Fe-species accelerate cathode and membrane degradation. Here, we interpret literature on single components to gain an understanding of how Fe-species influence low temperature CO_2 electrolyzers holistically. The role of Fe-species serves to highlight the need for considerations regarding component interplay in general.

1. Introduction

At the current rate of greenhouse gas emissions, a global warming of 1.5 °C above pre-industrial levels is expected by 2030.[1] Policies aiming at reducing the anthropogenic contribution towards climate change drive research and development of carbon capture and utilization technologies across all disciplines. The electrochemical reduction of CO_2 is a promising pathway to reduce emissions and close the carbon loop of various industrial processes. At high temperature (≥600 °C), the selective reduction of CO_2 to CO can be driven efficiently in electrolyzers that use solid oxide or molten carbonate electrolytes.[2] While operating less efficiently, low temperature electrolyzers that employ polymer electrolytes have the unique ability to directly convert CO_2 into a range of value-added products and useful chemicals such as ethylene, alcohols, or carboxylic acids.[2,3] Consequently, there has been a great deal of fundamental research on cell components and design with the intention of increasing efficiency and durability.[4] Moving forward, to ensure a smooth technological advancement of these promising devices, lessons learned from the previous development of related energy conversion devices should be implemented. For example, performance degradation observed in proton-conducting polymer-electrolyte-based fuel cells was identified and addressed comparably late into its technological development, delaying commercial implementation.[5] One likely explanation was the disconnect between testing environments and real application conditions.[5] For fast device development of CO_2 electrolyzers, stability under realistic conditions should be considered from the start.[6,7] An understanding of the respective cell components' requirements and consideration of the interplay between components is needed for durability to be appropriately assessed and addressed.

Two electrodes are needed for electrolysis, an anode that typically is used to drive the oxygen evolution reaction (OER) and a cathode where the CO_2 reduction reaction (CO_2RR) takes place. The electrodes are most often separated by an ion-conducting polymer electrolyte membrane. Metal electrocatalysts have shown the highest CO_2 conversion efficiencies. Impressive selectivity has been demonstrated for catalysts that form dominantly formic acid/formates (>95 %) or CO (>90 %).[3,4,8,9] High operating current densities exceeding 1 Acm^{-2} have even been attained at lower faradaic efficiency.[10–12] The lack of long-term stability, i.e. decrease in selectivity to carbon products and simultaneous increase of the competing hydrogen evolution reaction (HER) at the cathode remains a significant problem, and reports on CO_2 electrolysis systems exceeding 1,000 h in stability are rare.[13–16] Even the longest reported successful durability test by Kutz et al. at 4,380 h (6 months at 0.05 Acm^{-2}) is still far from what Kuengas predicted to be necessary to make the technology economically competitive, i.e. current densities of 1 Acm^{-2} and cell durability beyond 10,000 h, see Figure 1 red star.[2,15] Assuming 5 years of stable operation, Shin et al. report that different products would require different minimum current densities to be viable (≈0.1 Acm^{-2} for formic acid, ≈0.3 Acm^{-2} for CO and ethylene, or ≈0.6 Acm^{-2} for ethanol).[17] Jouny et al., assumed an even more optimistic

[*] Dr. A. F. Staerz, M. van Leeuwen, Dr. N. Plankensteiner, Dr. M. Jobbagy, S. Pahlavan, Dr. M. J. W. Blom, Dr. P. M. Vereecken
IMEC Leuven
Kapeldreef 75, 3001 Leuven (Belgium)
and
Energyville
Thor Park 8320, 3600 Genk (Belgium)
E-mail: astaerz@mines.edu

Dr. A. F. Staerz, M. van Leeuwen, Dr. N. Plankensteiner, S. Pahlavan, Dr. P. M. Vereecken
Department of Microbial and Micromolecular systems (M2S), cMACS,
KU Leuven
Celestijnenlaan 200F, 3001 Leuven (Belgium)

Dr. T. Priamushko, Dr. S. Cherevko
Forschungszentrum Jülich GmbH, Helmholtz-Institute Erlangen-Nürnberg for Renewable Energy (IEK-11)
Cauerstraße 1, 91058 Erlangen (Germany)

Dr. T. Saatkamp
Department of Chemistry, Simon Fraser University
8888 University Drive, Burnaby, British Columbia V5A 1S6 (Canada)

Dr. B. Endrődi, Dr. C. Janáky
Department of Physical Chemistry and Materials Science, University of Szeged
Rerrich sq. 1., 6720 Szeged (Hungary)

Dr. C. Janáky
eChemicles Zrt.
Alsó Kikötő sor 11, 6726 Szeged (Hungary)

Anna Staerz studied chemistry at the University of Tuebingen. She completed her PhD in the group of Prof. Weimar and Dr. Barsan during which she examined the surface chemistry of metal oxide gas sensors. Subsequently she studied solid oxide fuel cells as a postdoctoral associate in research group of Prof. Tuller at MIT and low temperature electrolysers in the group of Prof. Vereecken at imec. Since January 2023, she is an assistant professor at Colorado School of Mines in Metallurgical and Materials Engineering.

Marieke van Leeuwen obtained her M.Sc. In Chemical Engineering from Delft University of Technology. She currently works as a PhD student in the group of Prof. Vereecken at imec and the KU Leuven, under a FWO grant. Her research focuses on the development of novel gas diffusion electrodes for CO_2 electrolyzers.

Tatiana Priamushko studied solid state physics at the Tomsk Polytechnic University. She completed her Ph.D. in chemistry in the group of Prof. Freddy Kleitz at the University of Vienna. During her Ph.D., Tatiana studied non-noble mixed metal oxides as catalysts for the oxygen evolution reaction (OER). Since December 2021, she has been doing postdoctoral research in the group of Dr. Cherevko at Helmholtz Institute Erlangen-Nürnberg for Renewable Energy (HI ERN). The focus of her research is non-noble metal-based catalysts for the OER in a wide pH range.

Torben Saatkamp currently works as a postdoctoral fellow in Prof. Steven Holdcroft's group at SFU in Vancouver (Canada). His research focuses on the characterization of novel anion-conducting ionomers and membranes in CO_2 electrolyzers. Prior to this, Torben completed his PhD at the MPI for Solid State Research in Stuttgart (Germany), under the guidance of Dr. Klaus-Dieter Kreuer. His work there gave him an insight into fundamental structure–property relationships within cation and anion-conducting polymer electrolytes.

Balázs Endrődi obtained his PhD degree (2015) at the University of Szeged (Hungary). He was a postdoctoral researcher at KTH Stockholm (Sweden) between 2016–2018. In 2019 he returned to his Alma Mater, where he is currently working as an assistant professor. His research focus for the past years has been on applied electrochemical topics, most importantly on the electrochemical reduction of CO_2 and CO.

Nina Plankensteiner obtained her M.Sc. degree in Chemistry and Technology of Materials from Vienna University of Technology. She completed her PhD. on metal oxides for photovoltaics at the Austrian Institute of Technology and the University of Vienna under the supervision of Dr. Dimopoulos and Prof. Kautek in 2019. In 2020, she joined the energy storage & conversion group of Prof. Vereecken at imec and KULeuven, where works in the field of electrocatalysis, specifically focusing on materials for water electrolysis and CO_2 reduction.

Matias Jobbagy obtained his PhD (Inorganic Chemistry) at the University of Buenos Aires (UBA). After postdoctoral experiences and collaborations in Europe and Japan, he joined UBA as a professor. His research was focused on the use of mild chemistry to build and integrate hierarchical nanomaterials, including crystals, gels and monoliths, to be applied in energy, catalysis and biomedical fields. In 2020 he joined, as a researcher, the energy storage & conversion group of Prof. Vereecken at imec, where he is developing nano-hybrid electrolytes.

Sohrab Pahlavan is a second-year doctoral student at imec, energy storage and conversion, and KU Leuven, faculty of bioscience engineering. He is now working on electrocatalysts for alkaline fuel cells and water electrolysers. He acquired his masters in materials engineering from the Iran Ferdowsi university of Mashhad, working on localized corrosion of stainless steels; he studied his bachelor on materials and metallurgical engineering in the same university.

Martijn Blom obtained his PhD degree from the University of Twente in 2021. He is currently a researcher in the energy storage & conversion group of Prof. Vereecken at imec. Currently his research focus is on integrating novel electrolyzer components towards an ionically coupled system.

Csaba Janáky obtained his PhD degree (2011) at the University of Szeged (Hungary). He was a Marie Curie fellow at the UT Arlington (USA) between 2011–2014. He founded a research group at the University of Szeged in 2014, focusing on materials and energy orientated electrochemistry and photoelectrochemistry. Most recently, the focus has been on system level development and scale-up both for CO_2 electrolysis and hydrogen generation.

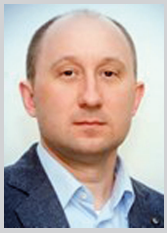

Serhiy Cherevko obtained his PhD degree in 2009 from Sungkyunkwan University in Suwon, Korea. Since 2016, he is the team head of the Electrochemical Energy Conversion group in the Helmholtz Institute Erlangen-Nürnberg for Renewable Energy. His research focus is the development of new tools, e.g. electrochemical on-line mass spectrometry, gas diffusion electrode approaches, and high-throughput screening methods, that can be used to gain a fundamnetal understanding of complex systems.

Philippe M. Vereecken is Fellow at imec and part-time professor at the University of Leuven (KU Leuven). He is Scientific director of the electrochemical storage and conversion activities at imec and EnergyVille. His main expertise lays in the combination of electrochemistry and nanomaterials and specifically in its use in semiconductors, electrocatalytic conversion, electrochemical storage and nanomaterials synthesis

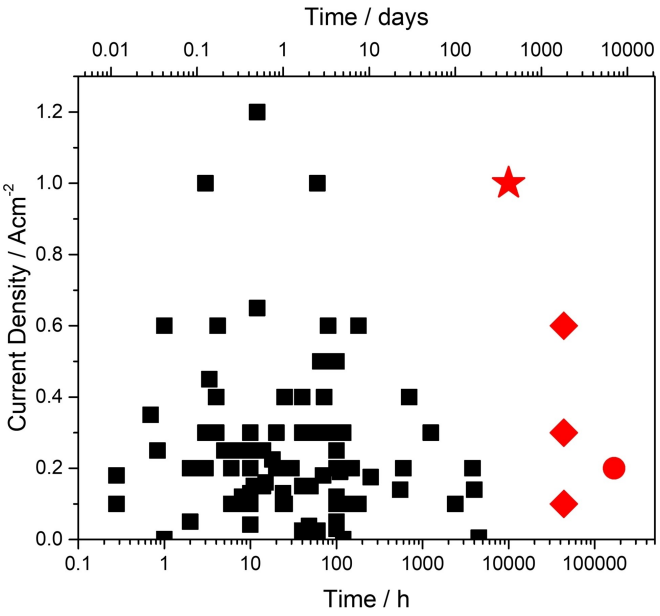

Figure 1. Summary of selected "application relevant" papers selected by Vass et al. and those subsequently published in which long-term stability was measured.[19] A complete summary of the papers can be found in the Supporting Information. As a comparison, the conditions cited by Kuengas as necessary to make low temperature CO_2 electrolysis competitive with other options are shown by the red star.[2] The requirements determined by Shin et al. are shown as red diamonds and for Jouny et. al as a red circle.[17,18] Please note for clarity the time axis is displayed logarithmically.

lifetime of 20 years (at 350 days of yearly operation) in their technoeconomic study (red circle).[18] These results are represented in Figure 1 as red diamonds, and are also above the current state of the art.

Many existing reviews focus on only one component of the electrolyzer.[19–22] From these it is clear that significant efforts have been invested to understand and increase performance or durability of single components. Now, however, to ensure practical applicability an understanding of the intricate interplay between cell components is needed.[14]

A large number of device parameters and component requirements are not yet clearly defined for low temperature CO_2 electrolysis and as a result widely varying solutions for single components have been explored. To streamline development, it is, however, crucial to avoid single component optimization that can inadvertently decrease the durability or performance of adjacent components in the full device. Due to its duplicitous effects within CO_2 electrolyzers, the role of iron is especially well suited to highlight the importance of holistic considerations during optimization. Fe-ions can originate from different sources within a typical CO_2 electrolysis cell.[23,24] This is problematic for durability, as already low concentrations ($\approx$1 ppm) can accelerate the degradation of the ionomers/membranes.[25,26] Even lower concentrations (hundreds of ppbs) have been found to influence electrode performance.[27,28] For example, the Faradaic efficiency of copper CO_2RR catalysts was found to decrease dramatically within hours due to Fe-impurities in the electrolyte.[27,28] At the same time, Fe-surface impurities reportedly enhance the activity of some catalysts' towards the OER.[29] As a result, iron has been deliberately added to the anolyte in recent studies, often neglecting the potentially detrimental effects on other cell components.[30] The response of researchers to the paradoxical influence of Fe-impurities, i.e., labor intensive steps to eliminate Fe-species and avoidance of stainless steel to study membrane and cathode materials, while intentionally adding them to increase the anode activity, underlines the importance of considering the interplay among the different cell components to realize stable systems in the future.

This conclusion is not too surprising, and we consider it to be broadly applicable to complex electrochemical systems. We have selected Fe-species due to their duplicitous nature but believe that the addition of new materials or potential contaminants into a system should always be considered holistically and across disciplines.

2. Basic Operation of a CO_2 Electrolysis Cell

Various cell designs have been studied—for a more in-depth overview, readers are referred to the works of Vass et al. and Garg et al.[19,31]

A brief summary of the different cell configurations is provided hereafter to equip readers from different fields with sufficient knowledge to understand how Fe-sources might affect the cell and its performance. In a classic H-cell configuration, both the cathode and the anode are immersed in a liquid electrolyte and a reference electrode is typically integrated close to the working electrode surface, to enable potential control. For scale-up, continuous flow reactors are advantageous as they allow increased mass transfer, better temperature and heat transfer control, and control of reaction mixture residence time in the reactor.[4] Numerous different configurations have been used for flow reactors. In the simplest case, the electrodes are in contact with separate liquid electrolytes (anolyte and catholyte) that are continuously flown through, and are separated by a membrane. In the scenario closest to H-cell conditions, CO_2 is dissolved in the catholyte. Although this is useful for basic research purposes, its real-world applicability is limited by the slow diffusion of CO_2 in water at ambient conditions.[2] Supplying gas-phase CO_2 to the cathode has been used to overcome mass transport limitations, see an overview of possible application relevant configurations in Figure 2. For this, the cathode electrocatalyst is immobilized on a gas diffusion layer (GDL) that is in contact with the catholyte on one side and the CO_2 on the other (Figure 2a). Variations of this cell have been studied. In zero-gap electrolyzer cells, both electrodes are pressed onto the separator. CO_2 is fed to the cathode side while a liquid electrolyte is fed to the anode side, see Figure 2b. The advantage of this configuration is that the two electrodes are close to one another, decreasing the overall cell resistance and due to their geometric similarity to PEM water electrolyzers, scale-up through large sized stacks seems feasible.[4] Microfluidic cells, in which the

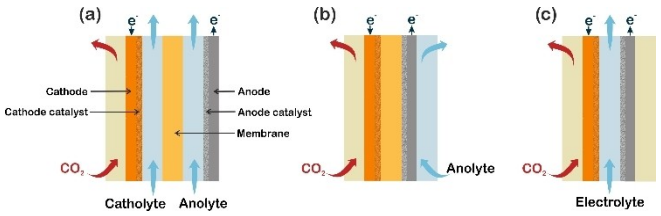

Figure 2. Schematic illustration of (a) a hybrid, (b) a membrane electrode assembly (MEA) and (c) a microfluidic electrolyzer for CO_2 reduction. These configurations are adapted from the perspective by Vass et al.[19]

electrodes are divided by a single small electrolyte channel (in the range of a few mm-s) have also been tested, Figure 2c.[4] Additional studies are needed to exam the upscaling potential of this configuration, e.g. does a longer electrolyte residence time in larger cells result in more product transport to the other electrode.[32]

While each cell configuration comes with its own caveats, in the following section the most important cell components will be generally introduced. Among the large number of publications on CO_2 electrolysis, application relevant electrodes, electrolyte and membranes, (> 0.1 Acm^{-2} and >50% Faradaic efficiency towards CO_2 reduction products), were selected based on reports from the past 5 years.[19] A complete summary of the papers can be found in the Supporting Information. Figure 3 shows an overview and summary graph of the used components.

2.1. Membrane

Both cation exchange membranes (CEM) and anion exchange membranes (AEM) have been tested for CO_2RR. CEMs are typically used in an acidic medium. They have a backbone that accommodates pendant negatively charged functional groups, such as sulfonic acid, carboxylic acid, or phosphonic acid groups. These groups enable the transport of positively charged mobile counter-ions (cations) e.g. potassium ions are transported through the membrane from the anode to the cathode (see Figure 3). In near neutral or

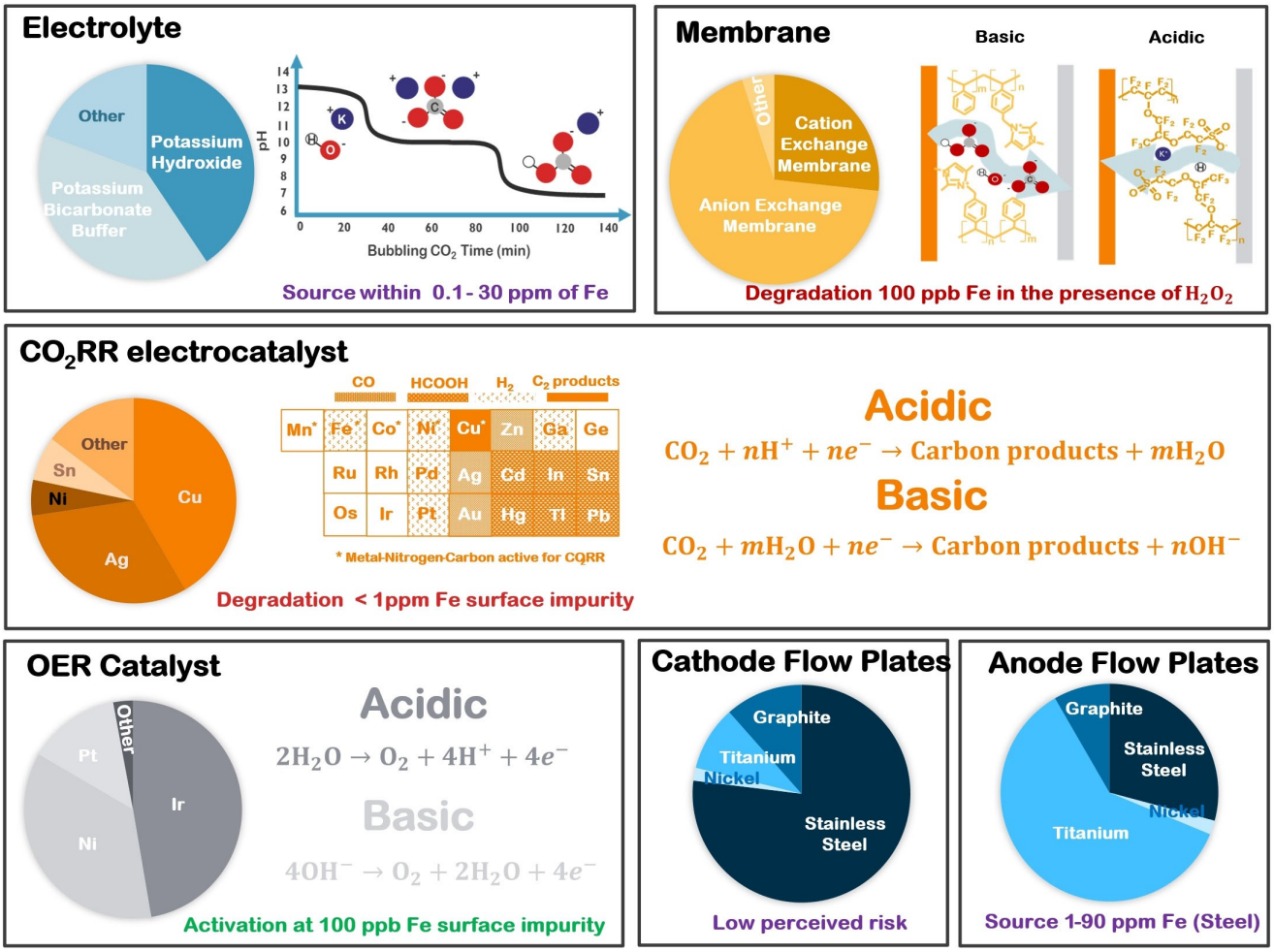

Figure 3. Summary of the central components in a low temperature CO_2 electrolyzer. The pie charts depict the frequency of different materials used in the papers selected by Vass et al. their review on Anodes and papers that were published subsequently.[19] The Fe-concentrations are approximations based on reports and are considered to be present in the electrolyte.

basic conditions, AEMs are more suitable.[20] AEMs contain fixed cationic groups, for example quaternary ammonium, phosphonium, or sulfonium units that allow the transport of negatively charged mobile anions. Bipolar membranes (BPMs), made up of a cation and an anion exchange layer, that facilitate the transport of H^+ to the cathode and OH^- to the anode through water dissociation, have also gained interest.[33]

2.2. Liquid Electrolyte

Depending on the cell setup, different electrolyte configurations have been reported; using both an anolyte and catholyte, only an anolyte or no electrolyte at all (only humidified gases). The most common liquid electrolyte is based on the potassium carbonate buffer system, see Figure 3. In some studies, constantly renewed potassium hydroxide is used as an electrolyte solution to maintain a high pH. In this case, the cell is not operating under steady state as purging with CO_2 will inevitably consume OH^- in the exergonic carbonate formation.[34] In other words, a bicarbonate buffer solution would be created on the cathode side over time. Furthermore, as a result of bicarbonate transport through the AEM, see Figure 3, neutralization of the recirculated anolyte is to be expected with time.[19,35] Typically, the pH upon CO_2 saturation of 1 M solution stabilizes at $\approx$7.5.[36] Beyond resulting in ill-defined measurement conditions, in situ neutralization has, often neglected, additional implications. For example, regenerating the hydroxide solution from the bicarbonate buffer would be energy intensive.[34] A very recent study, found that an even more complex model is needed to elucidate the true energetics of the system. In their study, Moore et al. considered the tradeoff between cell efficiency and gas separation. They find that when assuming the low energy requirements of industrial gas separation, the energy required for separating CO_2 from both O_2 produced at the anode and from the reduction products formed at the cathode, is negligible versus that needed for electrolysis. Furthermore they report that in the case where pure O_2 is produced at the anode, i.e. carbonate crossover is suppressed, the energetics are not necessarily better. For example, they argue that the increased expected cell voltage stemming from the use of a BPM would offset the better efficiency of the anode in basic conditions.[37] From these studies it is clear that determining the true energetics of CO_2 electrolysis is not trivial. Clearly, however, a prerequisite is that the system is stable in the steady state operation condition.

2.3. Electrodes

Different metals have been tested as CO_2RR electrocatalysts. They are commonly divided into four classes according to their dominant product: H_2 (Ni, Pd, Pt), HCOOH (In, Sn, Pb), CO (Zn, Ag, Au) or C_2 products and beyond (Cu). Copper and silver have become the preferred cathode materials for studies in application relevant conditions. While silver catalyzes the electroreduction of CO_2 to CO, copper is the only monometallic catalyst that can directly electrochemically reduce CO_2 into different high value and energy-dense products.[15,22,28] In the case of copper, typically a mix of products is attained as the standard reduction potentials of different CO_2 products are within a narrow range.[38] Unfortunately, the potential required to drive the competing HER is well within the general operating window for CO_2RR (-0.4 to -1 V vs RHE).[39] The most commonly used nickel-based electrocatalysts are single atom catalysts based on Ni–N–C.[40]

Depending on the expected conditions within a cell, different anode catalysts are employed. Acidic conditions are very harsh for the anodic catalyst and the reaction paired to CO_2RR is typically the electrochemical oxidation of water to form oxygen (i.e., OER).[41] Platinum and iridium are predominantly used in acidic and neutral cases.[19] One advantage of working in neutral or alkaline conditions is the possibility to use of non-noble OER catalysts, and Ni-based materials are being widely tested. Ageing and cycling in KOH has been found to significantly increase the reactivity, which is usually attributed to the formation of nickel (oxy)hydroxide.[30] Recently, however, this increased reactivity has been linked to surface Fe-impurities.[30,42] Although Ni-based OER catalysts are assumed stable in basic conditions, neutralization of the recirculated aqueous anolyte with time could compromise the catalyst's long-term stability.[19]

2.4. Porous Transport Layers

The multiphase interactions and transport between gas phase (e.g., densified CO_2, its gas-phase reduction products, and O_2), liquid phase (e.g., water, alcohols and higher hydrocarbon products and electrolytes) and solids (e.g., carbon, electro-catalysts, and ion conducting polymer) cause mass transport limitations at high reaction rates (i.e., current density).[43,44] To address these limitations, porous transport layers (PTLs), also called gas-diffusion layers (GDL) are used. PTLs also aid in creating good contact between adjacent components. On the anode side, PTLs made from titanium (acidic) or nickel (alkaline) are commonly used. On the cathode side, a dense network of carbon fibers such as carbon paper, carbon felt, or carbon cloth is typically implemented. When CO_2 is supplied as a humid gas, a hydrophobic modifier polytetrafluoroethylene (PTFE) is incorporated into carbon GDLs.[43,44]

2.5. Bipolar Plates

A key component of a CO_2 electrolyzer stacks are bipolar plates (BPPs) that connect individual cells in series (electrically). The BPPs provide mechanical stability to the stack and must have high electronic conductivity. As an example a MEA stack is schematically shown in, Figure 4, in which the bipolar plate is labeled. The plates are commonly equipped

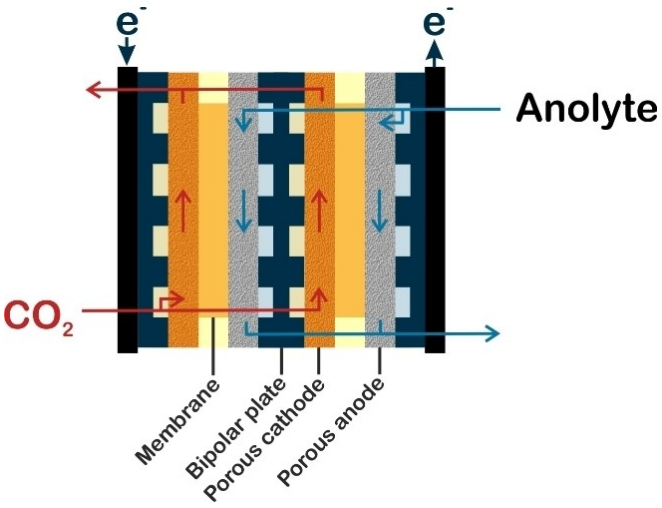

Figure 4. Schematic of an MEA-electrolyzer stack with parallel flow operation showing the main components including porous electrodes, membrane, bipolar plates and current collectors at the edges.

with channels on both sides to provide a uniform flow of solution/gases and facile removal of products. Finding a suitable material is not trivial. On the laboratory scale, due to the difference in requirements for the anodic and cathodic sides, different materials are often used. Titanium has become a popular choice for the anode plate (see Figure 3) as in near neutral/basic solutions and anodic conditions, it is passivated by a thin oxide layer. Although this passive oxide layer prevents further dissolution, it also increases the contact resistance.[45] In the case of the cathodic flow-plate, the probability of corrosion is lower and stainless steel (commonly 904 or 316), is already frequently implemented, see Figure 3. Stainless steel has significant advantages over titanium, e.g. high malleability enabling cheap fabrication of thin plates at scale.[24] Additionally, the costs of the raw materials in stainless steel are significantly lower than titanium, by about 20-fold.[45,46]

Due its significant advantages, the use of stainless steel for bipolar plates in electrolyzer stacks is likely. Although several studies have used steel flow plates on both sides, no study was found that specifically examines their durability during CO_2 electrolysis. Nonetheless, the Fe-impurities originating from uncoated anode plates, assuming a near neutral cycled bicarbonate buffer, can reasonably be expected to be between the max. 90 ppm determined by Novalin et al. in acidic fuel cell studies and the 2.5 ppm detected by Todoroki and Wadayama after cycling in 7 M KOH.[24,47]

3. Influence of Iron on the Individual Cell Components

Fe-impurities have been found to significantly influence the performance of different cell components. The degradation of different membranes due to Fe-impurities will be briefly reviewed. The reported changes in activity for both electrodes will be summarized, and existing mechanistic explanations will be provided.

3.1. Membranes

The unintended influence cationic impurities may have on CEMs is twofold. Firstly, in equilibrium, most cations have a higher affinity towards the sulfonate groups in the membrane than protons. When protons are replaced by other cations in the polymer structure, the hydrophilicity of the membrane is typically reduced due to the lower hydration enthalpies most sulfonate salts exhibit over their acid analogues.[48] This reduces the membrane's water uptake and affects its ionic conductivity.[48] Secondly, multivalent metal ion impurities, e.g., Fe^{3+}, can facilitate the chemical degradation of polymer electrolyte membranes, the most notable of which proceeds via the formation of aggressive radicals and is known as Fenton's degradation. It takes place in the presence of H_2O_2 and is accelerated at low pH. Under these conditions, highly oxidative radicals are formed via electron transfers between formed peroxide and iron impurities Figure 5.

The pathway for radical formation is described as:[49]

$$Fe^{2+} + H_2O_2 \rightarrow Fe^{3+} + OH^- + \bullet OH \quad (1)$$

or

$$Fe^{3+} + H_2O_2 \rightarrow Fe^{2+} + 2H^+ + \bullet OOH \quad (2)$$

H_2O_2 formation in fuel cells and electrolyzers originates from gas crossing over from one electrode to another through the membrane's aqueous-ionic domains and occurs on the catalytic surface.[50,51] Although gas crossover rates are slow, the chemical degradation of CEMs by means of radical attack can be catastrophic, and already low concentrations of Fe-ion impurities (100 ppb) have been found to be detrimental to CEMs in the presence of H_2O_2.[25,26] In devices, this mechanism leads to loss of membrane material and is observed e.g., in fuel cells as membrane thinning.[52]

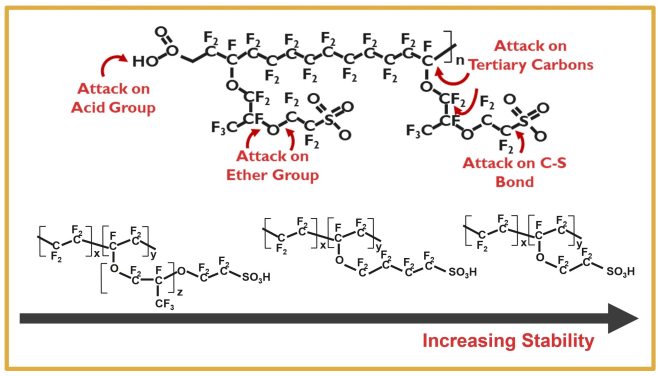

Figure 5. Degradation of CEMs.[53,54]

Mechanistically, Fenton-type degradation is initiated by the oxidizing species attacking either end group sites of the primary chain or sulfonic acid groups tethered to the polymeric backbone of a CEM, leading to bond cleavage and the propagation of defects.[53,54] The polymer's texture (porosity and tortuosity) and hydration level strongly affect the solubility and thus crossover rate of gases. Perfluorinated CEMs with an optimized chemical architecture, such as shorter side chains and avoidance of ether groups in their backbone as well as tertiary carbons in the side chain are marked by significantly higher stability against radical attack.[55,56] The design of modern CEMs avoids the use of perfluorinated materials which makes the materials more sustainable and allows for more flexible tuning of membrane properties. Due to safety concerns, perfluorinated materials are being widely phased out in Europe, making finding viable alternatives critical.[57] These new materials, however, often exhibit lower chemical and radical stability, highlighting the need to better understand this phenomenon in general.[58]

Anion exchange membranes (AEMs) consist typically of non-fluorinated polymer backbones that are comprised of fixed cationic groups and mobile anions as counter-ions, see Figure 6. In most applications (such as fuel cells or water electrolyzers), AEMs conduct hydrated hydroxide anions. In addition to susceptibility towards radical attack as seen in CEMs, AEMs must also withstand strongly alkaline conditions. Alkaline degradation is exacerbated when the membrane dries out (e.g., in fuel cells) or is exposed to highly alkaline media for extended periods of time at elevated temperature (e.g., in electrolyzers).[59,60] As a result, most studies focus primarily on the alkaline instability of AEMs. In the presence of iron, however, Fenton-type degradation superimposes these instabilities.[61] Substantial durability has been achieved by employing thick membranes, thus preventing gas crossover and avoiding radical formation in anion-exchange-membrane-based water electrolysis (AEMWE).[62,63] In most AEMWE studies, the use of 1 M KOH as a background electrolyte further masks the effect the potential degradation of functional groups of the polymeric separator has on system performances. Going forward, a more detailed post-mortem analysis of membranes should be conducted to elucidate the contributions of different chemicals, thermal and mechanical instabilities to degradation in these devices. In fuel cell application, where thin membranes (<20 μm) are commonly employed and no additional electrolyte is used, membranes and the ionomer in the catalyst layers need to be fully hydrated to avoid alkaline degradation. However, gas crossover under these conditions is facilitated, which can subsequentially lead to radical formation from intermediary H_2O_2 and trigger membrane degradation.[64] The main pathways of radical-driven degradation in common AEMs include phenyl group degradation by formation of phenolates, polymer backbone degradation, and quaternary ammonium cationic group degradation as highlighted in a recent review.[65] Some of the formed degradation products strongly resemble humic ligands.[66] These could in turn bind to iron ions and facilitate transport through the membrane or interact directly with the metallic electrode surface causing secondary degradation effects.[66]

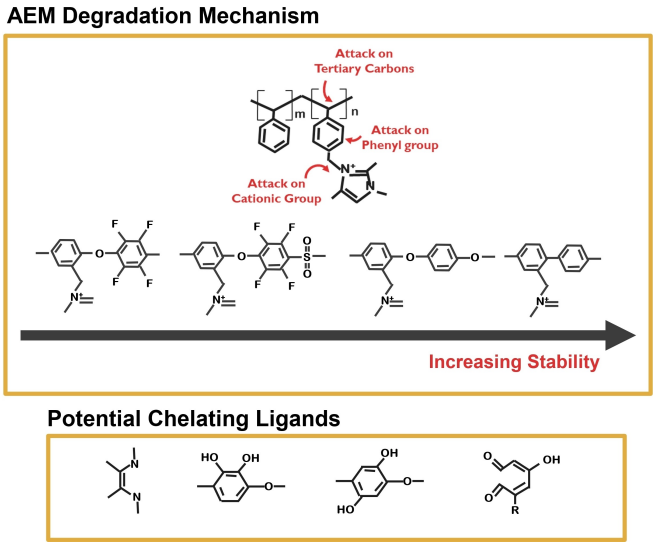

Figure 6. Degradation pathway of AEMs and examples of possible chelating ligands that are released as a result of the membrane degradation.[65,67]

The recent advancement of CO_2 electrolyzers, redox-flow batteries, and other electrochemical conversion devices has given rise to another, less studied material class, that of BPMs. In devices, BPMs can enable half-reactions to occur in different pH environments.[68] They consist of an AEM and CEM layer that are in direct contact, forming a bipolar junction. BPMs can be operated in reverse bias where in an aqueous environment water is split at the bipolar junction and hydroxide ions and protons migrate through the anion and cation conducting layer, respectively.[33] Under forward bias, the charge carrier ions recombine at the bipolar junction. This results in water formation in case of OH^- and H^+ conduction, but in CO_2 electrolyzers, as carbonate ions are the major charge carriers in the AEM, CO_2 evolves, distorting the BPM structure. Due to their similar chemical nature, the aforementioned degradation processes are relevant for bipolar membranes as well. In addition to radical and alkaline degradation, the dissimilar physical properties (e.g., swelling) of each hemi-membrane further tend to facilitate delamination, especially under forward bias, causing loss of conductivity at the interface.[21,69] In a bipolar membrane it is likely that degradation of the two sides will occur at different rates, which could accelerate other degradation processes, e.g. delamination. In general more research on gas crossover and degradation modes specific to BPMs is needed

3.2. Cathode

CO_2RR electrocatalyst degradation is generally attributed to 1) morphological changes, 2) impurity contamination or 3) surface poisoning by adsorption of carbon species.[22,70] Degradation due to changes in the catalyst structure has

received the greatest attention and is the focus of the recent review by Popovic et al.[22] Significant changes in catalyst morphology are reported when comparing CO_2RR electrocatalysts before and after use. Authors have attributed this to cathodic corrosion. Morphological changes under cathodic bias are highly debated.[71,72] An alternative explanation that has been offered is that morphological changes occur during the inevitable oxidizing periods before/after the measurement, namely during start-up and shut-down of the cell.[71,72] Cu-particles identified to be morphologically stable during CO_2 reduction, still showed degradation due to poisoning by extrinsic system impurities.[72] When working with low surface area submerged foils, Fe-contaminants in the liquid electrolyte have been found to be pervasive, already rapidly degrading low at ≈100 ppb.[73]

During CO_2RR, the impurity Fe-ions in the electrolyte could be reduced at the cathode to their metallic state.[74] This would likely occur in a stepwise process. Firstly, Fe^{3+} would be reduced to Fe^{2+}. Given the low solubility of Fe^{3+}, however, $Fe(OH)_3$ would likely be the dominant contaminant (even in solutions of pH 4 or 3). This contaminant would be expected to precipitate on the surface via:

$$Fe^{3+}(aq) + 3OH^-(aq) \rightarrow Fe(OH)_3(s) \quad (K_{sp} = 3.43 \cdot 10^{-38}) \tag{3}$$

In neutral and alkaline environments, even Fe^{2+} is unlikely to be in solution, and instead might precipitate as:

$$Fe^{2+}(aq) + 2OH^-(aq) \rightarrow Fe(OH)_2(s) \quad (K_{sp} = 9.07 \cdot 10^{-14}) \tag{4}$$

These precipitated hydroxides are expected to be reduced under the applied potential during typical electrolyzer operation via:

$$Fe(OH)_3(s) + e^- \rightarrow Fe(OH)_2(s) + OH^-(aq) \quad (U = 0.204\ V \text{ vs. RHE}) \tag{5}$$

$$Fe(OH)_2(s) + 2e^- \rightarrow Fe(s) + 2OH^-(aq) \quad (U = -0.088\ V \text{ vs. RHE}) \tag{6}$$

The presence of iron impurities could also increase the morphological changes that occur during the inevitable oxidizing periods before/after the measurement. The formation of copper-iron-oxides from interaction of $Fe(OH)_3$ with the native copper oxides could proceed as follows:

$$2Fe(OH)_3(s) + CuO \rightarrow CuO - Fe_2O_3(s) + 3H_2O \quad (K_{eq} = 1.04 \cdot 10^5) \tag{7}$$

or the even more thermodynamically favourable reaction with Cu_2O:

$$2Fe(OH)_3(s) + Cu_2O(s) \rightarrow Cu_2O - Fe_2O_3(s) + 3H_2O \quad (K_{eq} = 3.91 \cdot 10^{11}). \tag{8}$$

These oxides can easily mix and diffuse towards the metallic copper underneath where the reduction to metallic iron could proceed. These reactions serve as an examples of possible processes. Of course for completeness, depending on the used electrolyte, additional species must be considered, e.g. carbonates. The different degradation mechanisms are summarized in Figure 7.

Different mechanisms have been suggested to explain the significant degradation caused by Fe-surface impurities which are already detected far below the concentration needed for monolayer coverage, Figure 8.[73] Firstly, researchers argue that the iron ions preferentially adsorb onto the surface sites most reactive for CO_2 reduction, such as step-sites, grain boundaries, or certain reactive facets.[27,75] Secondly, beyond blocking reactive sites for CO_2 reduction, iron is known to catalyze the competing hydrogen evolution reaction.[73,76] This explanation is supported by the work of Kang et al. in which by selectively blocking surface Fe-sites using a metal–organic framework the CO_2RR efficiency of iron containing copper films was enhanced.[27,77–79]

3.3. Anode

As shown in Figure 3, the most widely used metallic anode catalysts are Pt, Ir, and Ni. The influence of Fe-impurities on Ir-based electrodes has not been studied in-depth. Recently, the behavior of Pt, Pd, and PtO_2, before and after adding K_2FeO_4 as a soluble source of iron has been investigated.[80,81] As Pt, Pd, and PtO_2 are all poor electrocatalysts for the OER, the authors suggested that they might act as a matrix for Fe-adsorption, leading to the formation of OER active sites. Moreover, Pt was concluded to be the best matrix for such purposes due to the formation of strong electronic interaction with Fe-ions.

Alternatively, even infinitesimally small amounts (sub-ppm in the electrolyte) of Fe-impurities present in KOH electrolytes are known to significantly alter the OER activity of Ni-based anodes.[30,82] The effect of Fe-impurities on Ni-containing OER catalysts was discovered in the 1980s and largely forgotten for nearly two decades.[83,84] Only recently

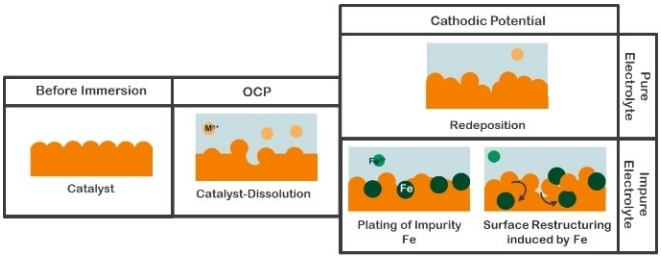

Figure 7. Schematic depicting the different ways in which the CO_2RR catalyst reacts with a pure and a Fe-contaminated electrolyte.

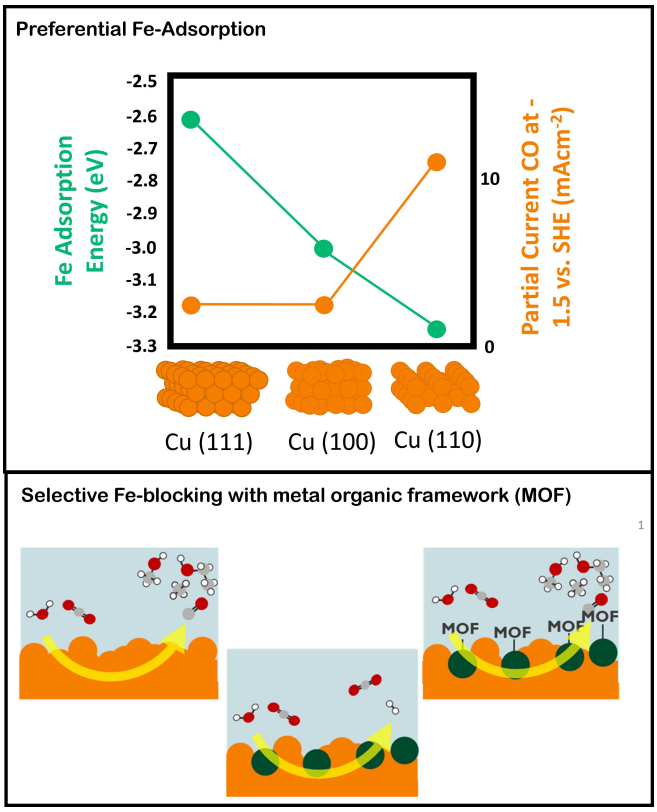

Figure 8. Schematic showing two ways in which low Fe-surface concentrations significantly influence the efficiency of the CO_2RR, (top) shows the preferential adsorption on particular surface site and the (bottom) shows the catalysis of the competing HER by Fe-surface species which was blocked using MOFs.[27,77–79]

has this topic regained attention. It has been suggested that Ni-anode's increased activity during ageing (soaking in KOH without applied potential) is due to the deposition of Fe-impurities on its surface.[23,30,42] Most studies report that cycling the electrode in a certain potential window results in the adsorption and incorporation of Fe-ions into the surface layers and sometimes also the bulk of Ni-containing catalysts. In addition to Ni, Co-based catalysts have received some attention as non-noble alternatives and a similar Fe-effect was found.[85] Usually, Fe-incorporation correlates with an anodic shift in the nominally +3/+2 and +4/+3 redox transformation of both Co- and Ni-based electrodes, indicating a strong electronic interaction between metals, see schematic illustration in Figure 9.[85,86] In addition to changing the anode's electronic structure,[29,42] Fe-impurities also form catalytically active adsorption sites,[23] and thereby affect its electrochemical activity toward the OER.[42,87]

3.4. Porous Transport Layers

There was no work found that specifically studied the influence of Fe-impurities on the porous transport layers (PTL). Here we will therefore rely on our understanding of the system and general information of degradation processes

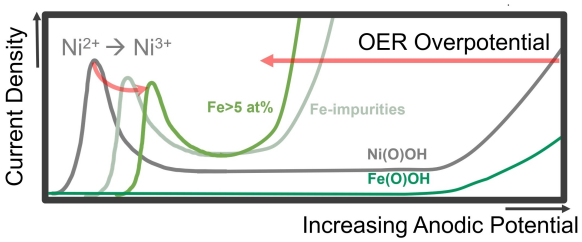

Figure 9. Schematic representation of the oxidation peaks of Ni and OER with respect to the Fe-impurity levels and the Fe content in the electrode material. While the effect of low concentrations notably lowers the OER overpotential, higher levels (e.g. 5 at%) result in negligible further enhancement.[42] Similar results were also reported for Co-based catalysts.[88]

to inform the reader of potential problems. The formation of oxidizing radical species (described in the membrane section in more detail) can be assumed to also accelerate the degradation of the carbon-based PTLs commonly used on the cathode side. Corrosion of the carbon layer could result in the loss of carbon content as well as the formation of surface oxides. Oxidation of the surface typically decreases its hydrophobicity. One of the commonly reported cell failure modes in application relevant systems summarized in Figure 3 is flooding. In this case, a fraction of the pores within the originally hydrophobic PTL is filled with the electrolyte solution (seeping through the membrane from the anolyte). As a result, CO_2 would have to diffuse through a liquid layer to reach the catalytic surface sites. Due to the low solubility of CO_2 in water the competing hydrogen evolution reaction becomes favorable.[89–91] Additionally, Fe-impurities could be deposited on the cathode PTL layer during electrolysis serving as catalytic sites for HER.

Titanium is a commonly used material for the PTLs of the anode side due to its perceived stability. With time, however, the oxide layer on the surface has been found to grow, which increases the contact resistance. This oxidation could presumably be accelerated in the presence of radicals.[92]

4. Sources of Iron and Avoidance Strategies

The significant effect of iron on the various cell components makes it apparent that the concentration of this impurity needs to be controlled throughout the whole CO_2RR electrolysis system. To deal with iron impurities during electrolysis, identification of potential contamination sources is of prime important. On the lab-scale, researchers often attribute the impurity simply to the chemicals used to prepare their electrolyte. Depending on the assembly and configuration of the electrochemical system, however, numerous other potential sources can be pinpointed. Iron can be unintentionally added during preparation from laboratory equipment, such as spatulas containing iron or contaminated glassware. During cell operation, additional sources could result in the continuous release of Fe-

impurities, such as the flow plates or even the electrodes themselves.[93] The different sources and possible remedies will be discussed here in more detail.

4.1. Electrolyte

Despite the use of high purity chemicals, aqueous electrolytes have been found to contain iron impurities, ranging from ppb to tens of ppm. Iron concentration within this range is enough to significantly influence the electrodes and the membrane.[22,73,94–96] Fe-impurities seem to be inherent to both potassium bicarbonate and hydroxide solutions, although their exact origin remains unclear. A recent article additionally highlighted significant batch-to-batch purity variation even for common chemicals.[97] Different methods have been developed to purify the electrolyte solution before use, see Figure 10. Both potassium bicarbonate and hydroxide have been successfully purified through electrolysis. For the purification of the bicarbonate buffer, commonly used as catholyte, high surface area electrodes of the same metal as the CO_2 electrocatalyst as well as Pt-black have been implemented.[73,94] For the anolyte it was found that after 25 h, no Fe-impurities in KOH were removed during electrolysis with a Ni-foam cathode.[96] Spanos et al. found, however, that by modifying the Ni foam with a MoS_2 catalyst, it is possible to remove the Fe-impurities within 10 h.[96]

Removal of impurities through electrolysis is tedious and energy intensive, i.e. requires upwards of 10 h, causing authors to explore other adsorption based purification methods. For the bicarbonate solutions, Wuttig and Surendranath therefore suggested using ethylenediaminetetraacetic acid (EDTA) to chelate impurities in situ.[94] A follow-up study by Jovanov et al. found that EDTA not only acts as an impurity scavenger, but also stabilizes the pH near the electrode, which could be the reason for the increased long-term stability.[98] As the chelating agent itself can also influence reaction pathways during CO_2 reduction, the ex situ treatment of the electrolyte with an ion exchange resin

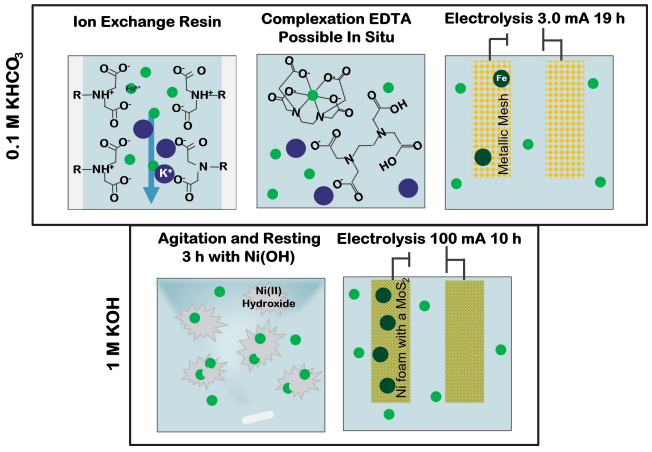

Figure 10. Schematic of different methods used to remove Fe-impurities from the electrolyte.[42,73,94,96]

may be better suited.[94] As a result, while these chelating methods are suitable for the near neutral pH bicarbonate buffer, for basic KOH solutions alternatives must be explored. Trotochaud et al. found that high-purity nickel hydroxide precipitate could be used as an Fe-absorbent for potassium hydroxide purification.[42,99] However, such purification techniques result in a Ni-contaminated electrolyte.[100] Generally, to ensure that the desired purity of the electrolyte is achieved before measurements, Márquez et al. recommends controlling impurity concentration using analytical tools e.g. ICP-MS.[97]

4.2. Electrodes

It is expected that if CO_2RR is carried out in neutral or even basic conditions, non-precious earth abundant catalysts could be used. As discussed above, recent results indicate that the OER activity reported for most Ni-, Co-, and even Mn-based oxides is high because of surface modification with iron.[23] Detecting low impurity concentrations on the surface of the electrode is not trivial. Clark et al. estimate that even ~20 % of monolayer can go undetected by XPS. The authors recommend using more surface-sensitive ion scattering spectroscopy.[101] Due to the seemingly high activity of iron for OER and the difficulties in detection, it is very likely that many reports of high OER activity, in fact, include the effect of Fe-impurities.

Authors have become interested in taking advantage of the "Fe-effect" to improve the catalytic activity of non-platinum group metals (non-PGM). Recently, there have been many reports of Ni–Fe composite OER electrodes or the use of higher Fe-concentrations in the electrolyte.[85,102,103] In general, studies have shown that small amounts of Fe-impurities in the electrolyte are more beneficial, while the "activation" of the catalysts has its limits. Xu et al. found that adding 1 mM $Fe(NO_3)_3$ into the alkaline electrolyte resulted in an immediate decrease of over 100 mV in the overpotential, while additionally doping Fe into the bulk had a negligible effect.[104] The viability of anodes making use of this Fe-effect remains unclear and additional testing in electrolyzers is needed.[104] Specifically, the stability of these "Fe-effect" anodes remains debated.

Despite the apparent similarity, crucial differences in the modes of Fe-incorporation into Co- and Ni-anodes have been identified.[42,85,86,105] Two types of Fe-incorporation into the anode catalyst were differentiated: intentional (co-deposition) and unintentional (Fe-incorporation from non-purified KOH electrolyte). At first, both materials showed similar behavior both $Co(Fe)O_x(OH)_y$ and $Ni(Fe)O_x(OH)_y$ prepared by co-deposition exhibited anodic shift of the cationic redox peak, indicating strong electronic interaction between metal ions. However, when Fe- impurities stemming from the electrolyte are involuntarily incorporated, the situation is different. The authors demonstrated that while Fe-ions can be easily incorporated into the surface and bulk of NiO_xH_y upon repeated cycling, they stay mostly on the surface and can't penetrate the bulk of CoO_xH_y. The ability of Fe to substitute Ni species in the bulk of NiO_xH_y was

explained by the weaker metal-oxygen bonds in comparison to CoO_xH_y. It seems that the structure of nickel oxyhydroxide is more dynamic, which allows such cation exchange processes. It was also found that the "surface Fe" quickly leaches from the catalyst upon cycling, while "bulk Fe" is more stable due to the strong electronic interactions.[42,85,86,105] Nonetheless, Speck et al. have found that when subjected to sustained electrolysis in strong base at 0.2 Acm^{-2}, most of the iron was liberated from the bulk Fe-doped Ni-anode during 24 h of operation.[106] Work by Tindall et al. also demonstrated instability and Fe-leaching from a NiFe layered double hydroxide (LDH)-based anode in a 1 M KOH-fed AEMWE. The authors conclude a more precise synthesis approach is needed to engineer stable metal centers in the NiFe LDHs.[107] Markovic's group report a dynamic stability of Fe i.e., it is continuously leached, adsorbed, and redeposited.[108] The authors studied the activity-stability trends in non-noble metal hydroxy oxides and found the dynamic stability results in acceptable performance.[63,109–111] This seems plausible for a closed system, but the authors did not specify what would occur when the Fe-species leaves the reaction zone.

Specific information on Fe-containing anodes in AEM-based CO_2 electrolyzers is needed to reveal the prevalent degradation pathways. Due to the local pH change and increasing concentration of carbonates on the anode side in CO_2 electrolyzers, Fe-dissolution from the catalyst might occur even more rapidly and prevent its redeposition. This decomposition of the anode could not only result in decreased OER activity but also serve as an additional source of Fe-impurities within the cell.

In conclusion, as even low iron concentrations have been found to influence a wide array of OER catalysts, it is currently difficult to deduce truly Fe-free anode materials. Studies are required in which impurities are closely monitored to ensure that the reported catalytic activity of the anode is not related to low levels of iron. Iron-free anode materials remain desirable as dynamic stability may not be sufficient for use in CO_2 electrolyzers due to the negative Fe-effect on other cell components.

4.3. Bipolar Plates and Porous Transport Layers

Among the various possible structural materials, stainless-steel, different grades of titanium and carbon structures are most widely implemented. Importantly, when selecting the raw materials for constructing electrolyzer cell components, the actual pH during operation is the most important factor to consider.[112] While an alkaline solution is typically fed to the anode at the beginning of the CO_2 electrolysis, if the anolyte is recirculated (and not regenerated continuously) its pH will decrease as a bicarbonate solution forms (at least in anion-exchange membrane-based cells).[36] This means that anodic plates should be formed of materials withstanding the oxidative potentials in near-neutral carbonate electrolytes (and not strong alkaline solutions, as in case of alkaline water electrolysis).

Titanium is the most widely used raw material for building electrolyzer cells (including the endplates and the bipolar plates). While titanium is definitely stable under cathodic conditions, its anodic oxidation leads to the formation of a non-conducting oxide layer. This oxide layer protects the surface from further oxidation but increases the cell resistance and consequently the cell voltage. To avoid this, a thin noble metal (e.g., Pt) layer is typically deposited onto it.[113] This process, on the other hand, increases the price notably. Also note, that even grade I titanium contains some small amount of alloying elements (maximum 0.03 % N, 0.1 % C, 0.015 % H, 0.2 % Fe, 0.18 % O), that might leach from it during extended operation. Due to the high surface area of PTLs, even low level Fe-leaching could be problematic. The iron content gradually increases with the titanium grade number up to 0.5 % for grade IV.[114]

Another alternative is applying carbon-based materials, just as in fuel-cells, where carbon gas diffusion layers are used at both the anode and the cathode. When the anode reaction in CO_2 electrolyzer cell is the oxidation of water to oxygen, however, the potential is already positive enough for carbon corrosion to occur. We envision that this could be suppressed by applying carbon-based composites, but these—to the best of our knowledge—have not yet been thoroughly studied in CO_2 electrolyzer cells.[115] We mention that this option might become realistic if an anode reaction occurring at less positive potential can be coupled with CO_2 reduction.[116]

A cost-efficient option (compared to high quality titanium) is stainless-steel. A wide range of different stainless-steel alloys are available, differing in their composition (alloying elements and their concentration), and hence in their (electro)chemical stability. The composition of some of the most frequently used stainless steel types (304 and 316, and their different variants) were summarized in Table 1. Notably, these stainless-steel types contain a fairly large amount of Cr and Ni (ca. 18 and 10 %, respectively). The leaching of these elements (and their subsequent deposition) could cause cell failure, and therefore this must be addressed when operating the electrolyzer cells. The major drawback of stainless-steel plates is their perceived potential for corrosion during operation. Nonetheless due to their advantages, there is a significant push to broadly integrate stainless steel bipolar plates in low temperature electrochemical cells, making their eventual use in CO_2 electrolyzers very likely.[53,117] No comprehensive studies were found that specifically examine the stability of stainless-steel interconnects and flow plates for CO_2 electrolysis. In our experience, 316Ti grade stainless steel is stable on the 100 h timescale under operating conditions, and longer

Table 1: Standard composition of different steels (wt%).

Type	C	Mn	Si	P	S	Cr	Mo	Ni	N	Other
304	0.07	2.00	0.75	0.045	0.03	17.5-19.5	-	8-10.5	0.1	
304L	0.03	2.00	0.75	0.045	0.03	17.5-19.5	-	8-10.5	0.1	
316	0.08	2.00	0.75	0.045	0.03	16.0-18.0	2.00-3.00	10.0-14.0	0.1	
316L	0.03	2.00	0.75	0.045	0.03	16.0-18.0	2.00-3.00	10.0-14.0	0.1	
316Ti	0.08	2.00	0.75	0.045	0.03	16.0-18.0	2.00-3.00	10.0-14.0	0.1	Ti ca. 0.70

measurements (coupled with periodic anolyte analysis) are in progress.[32]

4.4. Balance of Plant (BoP) Components

In general, once conditions and standard components for CO_2 electrolysers are identified, a robust measurement protocol should be developed.[118] An expansion of the databank of commonly used materials and standard test procedures developed for fuel cells by the US National Renewable Energy Lab would be highly useful.[119] Once a stable electrochemical cell stack is developed, the purity and influence of different BoP components can be considered.

The BoP components are not under electrochemical polarization when ionically decoupled from the stack, then only their chemical corrosion under process conditions must be considered. There is no single answer on the requirements for a given BoP component, as it is defined by many operational parameters together (i.e., pH, ionic strength, temperature). It is important to consider the composition of the given fluid stream which can get in contact with the given component. Also, very different BoP elements should be considered in the case of the different cell architectures (e.g., number of electrolytes, gas/liquid feed, etc.).[19] Therefore, it is part of the system development process to identify the proper elements.

Considering a system for operating a zero-gap electrolyzer cell, the pool of BoP components that can lead to contamination includes all system components from the gas-pre-treatment sub-system to the connection ports of the electrolyzer cell/stack (including the outlet) on the cathode side, and the total anolyte recirculation sub-system on the anode side, also including the connection ports on the cell (Figure 11). We go through the main components in what follows, see Figure 11.

The gas humidifier contains pure water at the beginning, but under operating conditions a mildly acidic pH develops because of CO_2 dissolution. This, especially at elevated temperatures, might corrode the typically used steel elements. The same is true for the pipes, delivering the humidified gas stream to the cell. This can be circumvented by using titanium, plastic (e.g., PTFE), or plastic-coated steel components. Typically neglected, but critical components are the connection ports, that must be also chosen with care. Here we emphasize that contact corrosion (galvanic corrosion) must be also considered—if the cell body, the piping and the connection port are of different material, high-rate local corrosion can be induced.[120]

As for the anolyte circuit, a mildly alkaline solution is delivered through a piping to and from the cell by a pump during operation, in most cases also passing through a heat exchanger (especially in case of larger systems). The parts that are in contact with the anolyte (anolyte container, piping, the inner parts of the cell and the heat exchanger and the connection ports) must withstand this pH and the operating temperature. Furthermore, the presence of oxygen creates a highly corrosive environment. High-quality stainless steel should in principle be suitable for this purpose, but this has not yet been confirmed during long operation. Additionally, steel is susceptible to localized corrosion.[121] An alternative would be using plastic or plastic-coated elements in the anolyte circuit.

Although zero-gap CO_2 electrolyzers build on the knowledge of the PEM water electrolysis community, there is a large difference in the operation of these different devices. In PEM water electrolyzers, a continuous, multi-step water ("anolyte") purification is employed, to remove any contaminant, coming either from the system or the stack. This is different in the CO_2 electrolysis case, as the contaminating cations have to be selectively removed from an electrolyte solution, necessitating the use of sophisticated ion-exchangers. Also, monitoring of the electrolyte contamination is not straightforward in this case. Analytical techniques must be applied to identify the different contaminants and determine their concentration, while a simple conductivity measurement is applied in case of PEM water electrolyzers.

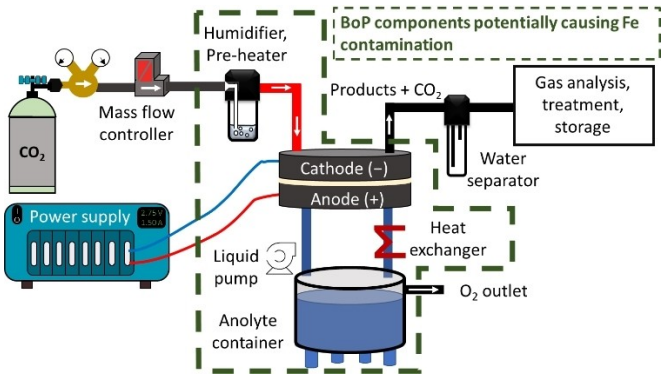

Figure 11. Simplified Process Flow Diagram of a zero-gap CO_2 electrolysis system. The BoP components that can potentially cause iron contamination are shown within the dashed green line.

5. Increasing Component Robustness against Fe-Impurities

Low levels of Fe-contamination within CO_2RR electrolyzers are likely unavoidable. As a result, increased stability of both the cathode and membrane against degradation is necessary. Different approaches have been examined in the literature, as are summarized in the following.

5.1. Membrane

In general, three different approaches have been implemented to increase the stability of the polymer electrolyte membranes: 1) preventing the formation of peroxide using a recombination catalyst, 2) adding a hydrogen peroxide decomposition catalyst and 3) using free radical scavengers.[122]

Firstly, recombination catalysts enable the reaction of permeated hydrogen back to water. Recombination cata-

lysts, e.g., Pt or Pt–Co, positioned within the membrane, on the anode porous transport layer, within the anodic catalyst layer or in an external gas exchanger have been found to significantly increase membrane stability in PEM fuel cells.[123–126]

Secondly, peroxide decomposition catalysts, such as Ag or MnO_2 have been studied. The catalytic behavior of materials is believed to be related to the ability of hydrogen peroxide to act both as an oxidizing and a reducing agent. The precise mechanism is still a matter of debate.[127–129]

Finally, free radical scavengers that decompose the reactive species have been successfully implemented. Specifically catalytic-type free radical scavengers are considered promising as they regenerate in situ. Different scavenger transition metals, such as cerium are commonly employed.[122] The relative ease of undergoing a reversible redox reaction between for example Ce^{3+} and Ce^{4+} states results in excellent scavenging properties.[122] The integration of radical scavengers into the membrane can, however, decrease ionic conductivity.[130] Additionally, the dissolution and subsequent migration of radical scavenger ions through the cell has been reported.[131–133] Stewart et al. examined the change in distribution of cerium cations, considering both initial immobilization on the membranes and in the cathode catalyst layer. They found that cerium cations are very mobile in CEMs and migrate into both the anode and cathode catalyst layer.[132] Yuk et al. report eleven-fold reduced dissolution rate of Ce^{4+} by coating ceria nanoparticles with a C_2N protective layer, while still increasing the stability of the membrane.[131]

In all cases, increasing the stability of the membrane involves the addition of metal ions to the system. This is, however, not without drawbacks and the effects on the whole cell should therefore be considered before implementation.

5.2. Cathode

There are four main methods in which extrinsic poisoning of the cathode is commonly combated, 1) periodic anodic stripping, 2) spiking of the electrolyte with catalyst ions, 3) using foreign-metal-induced restructuring and 4) high surface area catalysts, summarized in Figure 12.

Firstly, periodic anodic stripping of the poisons from the electrode's surface has been widely reported to increase long-term operability.[13,134–136] Anodization of the working electrode will, however, have effects beyond simply removing surface impurities. For example, authors reported increased surface roughness after anodization of copper as well as changes in the local chemical surroundings (e.g., pH or CO_2 concentration).[137,138] Additionally, changing the potential can also influence the passivation of stainless-steel flow plates, resulting in an overall increased Fe-concentration in the recirculated anolyte.

Secondly, a method similar to that used by Barwe et al. to enhance the stability of hydrogen evolution catalysts could be implemented in CO_2RR. The authors added catalyst ions to the electrolyte that deposited onto the cathode, regenerating the inactive surface layer.[93] This method is only applicable to configurations that have a catholyte. Additionally, potential catalyst ions, such as copper, have also been found to have Fenton activity, making their addition to the electrolyte potentially problematic for membrane stability.

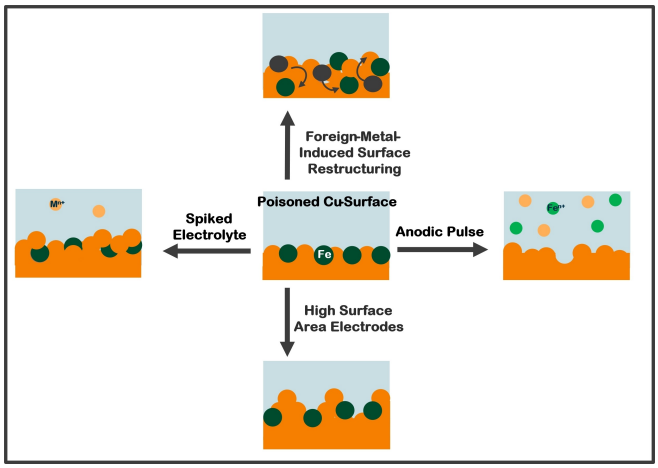

Figure 12. Schematic illustration of different methods used to combat poisoning of the cathode electrocatalyst by Fe-impurities.[79,93,136,139]

Thirdly, Weng et al. found that Pd deposition of Cu surface resulted in a surface instability, via continuous restructuring. The authors argue that as a result the catalyst surface is constantly regenerated, thereby maintaining its catalytic CO2RR properties during long-term operation ($\approx$16 h).[79] The mechanism was not elucidated by the authors. Surface reconstruction due to surface impurities is, however, a well known phenomenon in studies on under potential deposition (UPD), e.g. electrodeposition of a metal cation to a metal at a potential less negative than the equilibrium potential. Layers that have deposited via UPD are known to dive under the surface of the bulk material. The opposite mechanism is also possible..[140]

Finally, the seemingly most suitable method is to create high surface area cathode materials ("dimensionally stable cathodes"). Many authors have reported that nanostructured catalysts have increased stability, which Lu et al. attributes to their high surface area, because nanostructured electrocatalysts can accommodate much higher levels of impurities.[139] Clark et al. modeled how increasing the surface roughness will decrease the total level of unwanted surface coverage at different catholyte impurity concentrations.[101]

6. Outlook

The need for a technology that converts CO_2 into useful chemicals using clean energy from renewable resources is pressing. Low temperature electrolysis is a promising option in this regard. Due to the similar large-scale configuration, lessons can be learned from the more mature low temperature fuel cell and water electrolyzer technologies. From

these technologies, the need for stability and durability against common impurities becomes evident. Research on critical stability aspects is key for an accelerated successful large-scale technology implementation. The purpose of this review is twofold, it firstly uses the example of Fe-impurities in low temperature CO_2 electrolyzers, to highlight the need for proactive research in regard to stability. Secondly, this example more generally highlights the need to consider electrochemical systems holistically even when developing single components and cells.

Due to the ubiquitous nature of Fe-impurities, they are most likely unavoidable during CO_2 electrolysis. Therefore, existing methods of increasing the membrane and cathode stability against Fe-impurities must be expanded upon and new paths explored.

Based on this literature review it is clear that depending on the development level, e.g. small lab-scale versus full stack systems, the release of Fe-species from different components must be considered. From existing studies, the following inferences about when these sources will become important can be made (Figure 13). If a contaminated electrolyte is used, then there will be an initial Fe-impurity concentration. If the electrolyte is cycled, additional Fe-species from other sources can accumulate in the electrolyte over time. If iron containing cell hardware is used, it seems likely that the rate at which Fe-species are released will increase with time as corrosion processes intensify. This can either simply be due to more wear with time or changing conditions within the cell, e.g. anolyte neutralization. Finally, for larger scale systems, the BoP components must also be considered. Here there will likely be a delayed start, but if unsuitable materials are selected Fe-release will likely intensify with time as the system reaches the steady operation state, e.g. water in humidifier reaches mildly acidic pH because of CO_2 dissolution.

The more widespread monitoring and reporting of the Fe-concentration within electrolysis cells would allow these timescales to be better defined. When possible, the concentration of Fe- ions within the electrolyte and on the cathode determined in a post-mortem analysis should be included. Additionally, the cell housing components, e.g. composition of plates, should be standardly reported in the experimental section. Only this way can the true activity of the anode be determined for OER, corrosion processes be identified, and cathode degradation be clearly ascribed to a source. Once cell conditions are more clearly defined, a systematic study of intentionally added Fe-species at different concentrations would be very interesting and would e.g. be useful for determining suitable BOP components when upscaling.

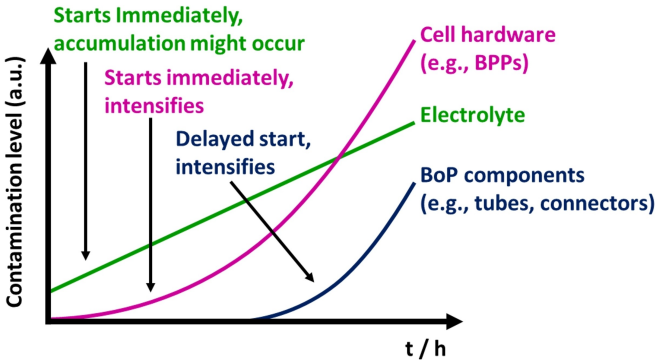

Figure 13. Schematic of the how Fe-release likely varies with time. Please note, more data must be collected to determine the exact function of release with time.

Our study also highlights why the entire electrochemical system needs to be considered when developing single cell and system components. Although there is a great fervor surrounding CO_2RR, currently most research concentrates on the optimization of only one cell component (e.g., design of catalyst cathodes, fabrication of novel membranes). This has led to the situation in which highly optimized cathodes and membranes work best in the total absence of Fe-impurities while non-noble anode materials are often reliant on them. This paradox lays bare the issues with single component optimization and highlights the need for a more holistic research approach. We feel that in order to enable the accelerated innovation necessary to address the pressing energy needs, even lab scale research should be mindful of the interplay between components. We believe this conclusion is generally relevant for optimization of complex electrochemical systems.

Supporting Information

The authors have cited additional references within the Supporting Information.[10,15,79,112,141–258]

Acknowledgements

MvL gratefully acknowledges the support of the PhD fellowship (Grant No. 1SD5923N) from the Research Foundation Flanders (FWO). CJ and EB acknowledges the Hungarian support through the project no. RRF-2.3.1-21-2022-00009, titled National Laboratory for Renewable Energy has been implemented with the support provided by the Recovery and Resilience Facility of the European Union within the framework of Programme Széchenyi Plan Plus. NP acknowledges funding from the European Union's Horizon 2020 research and innovation programme under the Marie Sklodowska Curie Individual Felllowship (No. 101032191). TS acknowledges postdoctoral fellowship funding through the National Research Council Canada's Materials for Clean Fuels Challenge Program (Collaborative Research Agreement: MCF-103-1).

Conflict of Interest

The authors declare no conflict of interest.

Data Availability Statement

Data sharing is not applicable to this article as no new data were created or analyzed in this study.

Keywords: CO_2RR · Contamination · Degradation · Electrolysis · Fe-Effect

[1] "That's how fast the carbon clock is ticking," can be found under https://www.mcc-berlin.net/en/research/co2-budget.html.

[2] R. Küngas, *J. Electrochem. Soc.* **2020**, *167*, 044508.

[3] S. Nitopi, E. Bertheussen, S. B. Scott, X. Liu, A. K. Engstfeld, S. Horch, B. Seger, I. E. L. Stephens, K. Chan, C. Hahn, J. K. Nørskov, T. F. Jaramillo, I. Chorkendorff, *Chem. Rev.* **2019**, *119*, 7610–7672.

[4] B. Endrődi, G. Bencsik, F. Darvas, R. Jones, K. Rajeshwar, C. Janáky, *Prog. Energy Combust. Sci.* **2017**, *62*, 133–154.

[5] F. N. Büchi, T. J. Schmidt, M. Inaba, *Polymer Electrolyte Fuel Cell Durability*, Springer, New York, New York, NY, **2009**.

[6] T. Holmes, T. J. G. Skalski, M. Adamski, S. Holdcroft, *Chem. Mater.* **2019**, *31*, 1441–1449.

[7] S. Cherevko, *Curr. Opin. Electrochem.* **2018**, *8*, 118–125.

[8] J. Li, H. Zeng, X. Dong, Y. Ding, S. Hu, R. Zhang, Y. Dai, P. Cui, Z. Xiao, D. Zhao, L. Zhou, T. Zheng, J. Xiao, J. Zeng, C. Xia, *Nat. Commun.* **2023**, *14*, 340.

[9] A. Alihosseinzadeh, A. Unnikrishnan, K. Karan, S. Ponnurangam, *ACS Appl. Energ. Mater.* **2023**, *6*, 1533–1543.

[10] C. T. Dinh, T. Burdyny, G. Kibria, A. Seifitokaldani, C. M. Gabardo, F. Pelayo García De Arquer, A. Kiani, J. P. Edwards, P. De Luna, O. S. Bushuyev, C. Zou, R. Quintero-Bermudez, Y. Pang, D. Sinton, E. H. Sargent, *Science* **2018**, *360*, 783–787.

[11] Z. Liu, H. Yang, R. Kutz, R. I. Masel, *J. Electrochem. Soc.* **2018**, *165*, J3371–J3377.

[12] F. P. García de Arquer, C.-T. Dinh, A. Ozden, J. Wicks, C. McCallum, A. R. Kirmani, D.-H. Nam, C. Gabardo, A. Seifitokaldani, X. Wang, Y. C. Li, F. Li, J. Edwards, L. J. Richter, S. J. Thorpe, D. Sinton, E. H. Sargent, *Science* **2020**, *367*, 661.

[13] A. Engelbrecht, C. Uhlig, O. Stark, M. Hämmerle, G. Schmid, E. Magori, K. Wiesner-Fleischer, M. Fleischer, R. Moos, *J. Electrochem. Soc.* **2018**, *165*, J3059–J3068.

[14] I. E. L. Stephens, K. Chan, A. Bagger, S. W. Boettcher, J. Bonin, E. Boutin, A. K. Buckley, R. Buonsanti, E. R. Cave, X. Chang, S. W. Chee, A. H. M. da Silva, P. de Luna, O. Einsle, B. Endrődi, M. Escudero-Escribano, J. V. Ferreira de Araujo, M. C. Figueiredo, C. Hahn, K. U. Hansen, S. Haussener, S. Hunegnaw, Z. Huo, Y. J. Hwang, C. Janáky, B. S. Jayathilake, F. Jiao, Z. P. Jovanov, P. Karimi, M. T. M. Koper, K. P. Kuhl, W. H. Lee, Z. Liang, X. Liu, S. Ma, M. Ma, H.-S. Oh, M. Robert, B. R. Cuenya, J. Rossmeisl, C. Roy, M. P. Ryan, E. H. Sargent, P. Sebastián-Pascual, B. Seger, L. Steier, P. Strasser, A. S. Varela, R. E. Vos, X. Wang, B. Xu, H. Yadegari, Y. Zhou, *J. Phys. E* **2022**, *4*, 042003.

[15] R. B. Kutz, Q. Chen, H. Yang, S. D. Sajjad, Z. Liu, I. R. Masel, *Energy Technol.* **2017**, *5*, 929–936.

[16] K. Xiang, F. Zhu, Y. Liu, Y. Pan, X. Wang, X. Yan, H. Liu, *Electrochem. Commun.* **2019**, *102*, 72–77.

[17] H. Shin, K. U. Hansen, F. Jiao, *Nat. Sustainability* **2021**, *4*, 911–919.

[18] M. Jouny, W. Luc, F. Jiao, *Ind. Eng. Chem. Res.* **2018**, *57*, 2165–2177.

[19] Á. Vass, A. Kormányos, Z. Kószo, B. Endrődi, C. Janáky, *ACS Catal.* **2022**, *12*, 1037–1051.

[20] D. A. Salvatore, C. M. Gabardo, A. Reyes, C. P. O'Brien, S. Holdcroft, P. Pintauro, B. Bahar, M. Hickner, C. Bae, D. Sinton, E. H. Sargent, C. P. Berlinguette, *Nat. Energy* **2021**, *6*, 339–348.

[21] P. K. Giesbrecht, M. S. Freund, *Chem. Mater.* **2020**, *32*, 8060–8090.

[22] S. Popović, M. Smiljanić, P. Jovanovič, J. Vavra, R. Buonsanti, N. Hodnik, *Angew. Chem. Int. Ed.* **2020**, *59*, 14736–14746.

[23] I. Spanos, J. Masa, A. Zeradjanin, R. Schlögl, *Catal. Lett.* **2021**, *151*, 1843–1856.

[24] T. Novalin, B. Eriksson, S. Proch, U. Bexell, C. Moffatt, J. Westlinder, C. Lagergren, G. Lindbergh, R. W. Lindström, *Int. J. Hydrogen Energy* **2021**, *46*, 13855–13864.

[25] S. H. Frensch, G. Serre, F. Fouda-Onana, H. C. Jensen, M. L. Christensen, S. S. Araya, S. K. Kær, *J. Power Sources* **2019**, *420*, 54–62.

[26] P. Frühwirt, A. Kregar, J. T. Törring, T. Katrašnik, G. Gescheidt, *Phys. Chem. Chem. Phys.* **2020**, *22*, 5647–5666.

[27] D. H. Won, H. Shin, M. W. Chung, H. Jung, K. H. Chae, H.-S. Oh, Y. J. Hwang, B. K. Min, *Appl. Catal. B* **2019**, *258*, 117961.

[28] T. Haas, R. Krause, R. Weber, M. Demler, G. Schmid, *Nat. Catal.* **2018**, *1*, 32–39.

[29] S. Klaus, Y. Cai, M. W. Louie, L. Trotochaud, A. T. Bell, *J. Phys. Chem. C* **2015**, *119*, 7243–7254.

[30] S. Anantharaj, S. Kundu, S. Noda, *Nano Energy* **2021**, *80*, 105514.

[31] S. Garg, M. Li, A. Z. Weber, L. Ge, L. Li, V. Rudolph, G. Wang, T. E. Rufford, *J. Mater. Chem. A* **2020**, *8*, 1511–1544.

[32] A. A. Samu, A. Kormányos, E. Kecsenovity, N. Szilágyi, B. Endrődi, C. Janáky, *ACS Energy Lett.* **2022**, *7*, 1859–1861.

[33] R. Pärnamäe, S. Mareev, V. Nikonenko, S. Melnikov, N. Sheldeshov, V. Zabolotskii, H. V. M. Hamelers, M. Tedesco, *J. Membr. Sci.* **2021**, *617*, 118538.

[34] J. A. Rabinowitz, M. W. Kanan, *Nat. Commun.* **2020**, *11*, 5231.

[35] P. Mardle, S. Cassegrain, F. Habibzadeh, Z. Shi, S. Holdcroft, *J. Phys. Chem. C* **2021**, *125*, 25446–25454.

[36] Z. Rastegar, A. Ghaemi, *Heat Mass Transfer* **2022**, *58*, 365–381.

[37] T. Moore, D. I. Oyarzun, W. Li, T. Y. Lin, M. Goldman, A. A. Wong, S. A. Jaffer, A. Sarkar, S. E. Baker, E. B. Duoss, C. Hahn, *Joule* **2023**, *7*, 782–796.

[38] Z. Sun, T. Ma, H. Tao, Q. Fan, B. Han, *Chem* **2017**, *3*, 560–587.

[39] A. Goyal, G. Marcandalli, V. A. Mints, M. T. M. Koper, *J. Am. Chem. Soc.* **2020**, *142*, 4154–4161.

[40] A. S. Varela, W. Ju, A. Bagger, P. Franco, J. Rossmeisl, P. Strasser, *ACS Catal.* **2019**, *9*, 7270–7284.

[41] Q. Liang, G. Brocks, A. Bieberle-Hütter, *J. Phys. E* **2021**, *3*, 026001.

[42] L. Trotochaud, S. L. Young, J. K. Ranney, S. W. Boettcher, *J. Am. Chem. Soc.* **2014**, *136*, 6744–6753.

[43] Z. Kang, S. M. Alia, J. L. Young, G. Bender, *Electrochim. Acta* **2020**, *354*, 136641.

[44] A. Gawel, T. Jaster, D. Siegmund, J. Holzmann, H. Lohmann, E. Klemm, U.-P. Apfel, *iScience* **2022**, *25*, 104011.

[45] R. K. Gautam, S. Banerjee, K. K. Kar, *Recent Pat. Mater. Sci.* **2015**, *8*, 15–45.

[46] K. E. Ayers, E. B. Anderson, C. B. Capuano, M. Niedzwiecki, M. A. Hickner, C.-Y. Wang, Y. Leng, W. Zhao, *ECS Trans.* **2013**, *45*, 121–130.

[47] N. Todoroki, T. Wadayama, *Int. J. Hydrogen Energy* **2022**, *47*, 32753–32762.

[48] G. Xie, T. Okada, *J-Stage* **1996**, *64*, 718–726.

[49] V. O. Mittal, H. R. Kunz, J. M. Fenton, *J. Electrochem. Soc.* **2006**, *153*, A1755.

[50] U. Babic, M. Suermann, F. N. Büchi, L. Gubler, T. J. Schmidt, *J. Electrochem. Soc.* **2017**, *164*, F387–F399.
[51] S. J. Paddison, H. A. Gasteiger, in *Encyclopedia of Sustainability Science and Technology*, Springer, New York, New York, NY, **2012**, pp. 7756–7777.
[52] T. Novalin, B. Ericksson, S. Proch, U. Bexell, C. Moffat, J. Westlinder, C. Lagergren, G. Lindbergh, R. Wreland Lindstroem, *Energy Convers. Manage.* **2022**, *253*, 115153.
[53] A. Hermann, T. Chaudhuri, P. Spagnol, *Int. J. Hydrogen Energy* **2005**, *30*, 1297–1302.
[54] A. B. LaConti, M. Hamdan, R. C. McDonald, in *Handbook of Fuel Cells*, John Wiley & Sons, Ltd, Hoboken, **2010**.
[55] L. Ghassemzadeh, K. D. Kreuer, J. Maier, K. Müller, *J. Phys. Chem. C* **2010**, *114*, 14635–14645.
[56] M. Danilczuk, A. J. Perkowski, S. Schlick, *Macromolecules* **2010**, *43*, 3352–3358.
[57] *ECHA/NR/23/04*, Helsinki, **2023**.
[58] L. Gubler, S. M. Dockheer, W. H. Koppenol, *J. Electrochem. Soc.* **2011**, *158*, B755–B769.
[59] N. Chen, Y. M. Lee, *Prog. Polym. Sci.* **2021**, *113*, 101345.
[60] S. Gottesfeld, D. R. Dekel, M. Page, C. Bae, Y. Yan, P. Zelenay, Y. S. Kim, *J. Power Sources* **2018**, *375*, 170–184.
[61] G. A. Lindquist, Q. Xu, S. Z. Oener, S. W. Boettcher, *Joule* **2020**, *4*, 2549–2561.
[62] M. Moreno-González, P. Mardle, S. Zhu, B. Gholamkhass, S. Jones, N. Chen, B. Britton, S. Holdcroft, *J. Power Sources Advances* **2023**, *19*, 100109.
[63] B. Motealleh, Z. Liu, R. I. Masel, J. P. Sculley, Z. Richard Ni, L. Meroueh, *Int. J. Hydrogen Energy* **2021**, *46*, 3379–3386.
[64] S. Wierzbicki, J. C. Douglin, A. Kostuch, D. R. Dekel, K. Kruczała, *J. Phys. Chem. Lett.* **2020**, *11*, 7630–7636.
[65] D. Li, A. R. Motz, C. Bae, C. Fujimoto, G. Yang, F. Y. Zhang, K. E. Ayers, Y. S. Kim, *Energy Environ. Sci.* **2021**, *14*, 3393–3419.
[66] E. Orlowska, A. Roller, M. Pignitter, F. Jirsa, R. Krachler, W. Kandioller, B. K. Keppler, *Sci. Total Environ.* **2017**, *577*, 94–104.
[67] D. Henkensmeier, M. Najibah, C. Harms, J. Žitka, J. Hnát, K. Bouzek, *J. Electrochem. Energy Convers. Storage* **2021**, *18*, 024001.
[68] J. B. Mitchell, L. Chen, K. Langworthy, K. Fabrizio, S. W. Boettcher, *ACS Energy Lett.* **2022**, *7*, 3967–3973.
[69] M. A. Blommaert, D. Aili, R. A. Tufa, Q. Li, W. A. Smith, D. A. Vermaas, *ACS Energy Lett.* **2021**, *6*, 2539–2548.
[70] W. Choi, D. H. Won, Y. J. Hwang, *J. Mater. Chem. A* **2020**, *8*, 15341–15357.
[71] T. Wirtanen, T. Prenzel, J. P. Tessonnier, S. R. Waldvogel, *Chem. Rev.* **2021**, *121*, 10241–10270.
[72] S. J. Raaijman, N. Arulmozhi, M. T. M. Koper, *ACS Appl. Mater. Interfaces* **2021**, *13*, 48730–48744.
[73] Y. Hori, H. Konishi, T. Futamura, A. Murata, O. Koga, H. Sakurai, K. Oguma, *Electrochim. Acta* **2005**, *50*, 5354–5369.
[74] E. Herrero, L. J. Buller, H. D. Abruña, *Chem. Rev.* **2001**, *101*, 1897–1930.
[75] D. Cheng, Z.-J. Zhao, G. Zhang, P. Yang, L. Li, H. Gao, S. Liu, X. Chang, S. Chen, T. Wang, G. A. Ozin, Z. Liu, J. Gong, *Nat. Commun.* **2021**, *12*, 395.
[76] X. Li, C. M. Gunathunge, N. Agrawal, H. Montalvo-Castro, J. Jin, M. J. Janik, M. M. Waegele, *J. Electrochem. Soc.* **2020**, *167*, 106505.
[77] N. Hoshi, M. Kato, Y. Hori, *J. Electroanal. Chem.* **1997**, *440*, 283–286.
[78] S. J. Kang, J. H. Won, H. Choi, W. Sim, M. K. Kim, S. Sultan, Y. Kwon, H. M. Jeong, *J. Energy Chem.* **2022**, *66*, 68–73.
[79] Z. Weng, X. Zhang, Y. Wu, S. Huo, J. Jiang, W. Liu, G. He, Y. Liang, H. Wang, *Angew. Chem.* **2017**, *129*, 13315–13319.
[80] A. Valizadeh, P. Aleshkevych, M. M. Najafpour, *Inorg. Chem.* **2022**, *61*, 613–621.
[81] N. Akbari, I. Kondov, M. Vandichel, P. Aleshkevych, M. M. Najafpour, *Inorg. Chem.* **2021**, *60*, 5682–5693.
[82] D. A. Corrigan, *J. Electrochem. Soc.* **1983**, *134*, 2125.
[83] D. A. Corrigan, *The Catalysis of the Oxygen Evolution Reaction by Iron Impurities in Thin Film Nickel Oxide Electrodes*, Cambridge University Press, **1983**.
[84] G. Młynarek, M. Paszkiewicz, A. Radniecka, *J. Appl. Electrochem.* **1984**, *14*, 145–149.
[85] M. S. Burke, M. G. Kast, L. Trotochaud, A. M. Smith, S. W. Boettcher, *J. Am. Chem. Soc.* **2015**, *137*, 3638–3648.
[86] M. B. Stevens, C. D. M. Trang, L. J. Enman, J. Deng, S. W. Boettcher, *J. Am. Chem. Soc.* **2017**, *139*, 11361–11364.
[87] C. Dette, M. R. Hurst, J. Deng, M. R. Nellist, S. W. Boettcher, *ACS Appl. Mater. Interfaces* **2019**, *11*, 5590–5594.
[88] M. S. Burke, S. Zou, L. J. Enman, J. E. Kellon, C. A. Gabor, E. Pledger, S. W. Boettcher, *J. Phys. Chem. Lett.* **2015**, *6*, 3737–3742.
[89] K. Yang, R. Kas, W. A. Smith, T. Burdyny, *ACS Energy Lett.* **2021**, *6*, 33–40.
[90] L. Castanheira, W. O. Silva, F. H. B. Lima, A. Crisci, L. Dubau, F. Maillard, *ACS Catal.* **2015**, *5*, 2184–2194.
[91] Y. Pan, H. Wang, N. P. Brandon, *J. Power Sources* **2021**, *513*, 230560.
[92] M. Prestat, *J. Power Sources* **2023**, *556*, 232469.
[93] S. Barwe, B. Mei, J. Masa, W. Schuhmann, E. Ventosa, *Nano Energy* **2018**, *53*, 763–768.
[94] A. Wuttig, Y. Surendranath, *ACS Catal.* **2015**, *5*, 4479–4484.
[95] D. W. DeWulf, T. Jin, A. J. Bard, *J. Electrochem. Soc.* **1989**, *136*, 1686–1692.
[96] I. Spanos, M. F. Tesch, M. Yu, H. Tüysüz, J. Zhang, X. Feng, K. Müllen, R. Schlögl, A. K. Mechler, *ACS Catal.* **2019**, *9*, 8165–8170.
[97] R. A. Márquez, K. Kawashima, Y. J. Son, G. Castelino, N. Miller, L. A. Smith, C. E. Chukwuneke, C. B. Mullins, *ACS Energy Lett.* **2023**, *8*, 1141–1146.
[98] Z. P. Jovanov, J. Ferreira De Araujo, S. Li, P. Strasser, *J. Phys. Chem. C* **2019**, *123*, 2165–2174.
[99] A. Dutta, A. K. Samantara, S. K. Dutta, B. K. Jena, N. Pradhan, *ACS Energy Lett.* **2016**, *1*, 169–174.
[100] L. Liu, L. P. Twight, J. L. Fehrs, Y. Ou, D. Sun, S. W. Boettcher, *ChemElectroChem* **2022**, *9*, e202200279.
[101] E. L. Clark, J. Resasco, A. Landers, J. Lin, L. T. Chung, A. Walton, C. Hahn, T. F. Jaramillo, A. T. Bell, *ACS Catal.* **2018**, *8*, 6560–6570.
[102] N. Hashemi, S. Nandy, K. H. Chae, M. M. Najafpour, *ACS Appl. Energ. Mater.* **2022**, *5*, 11098–11112.
[103] W. Moschkowitsch, N. Zion, H. C. Honig, N. Levy, D. A. Cullen, L. Elbaz, *ACS Catal.* **2022**, *12*, 12162–12169.
[104] D. Xu, M. B. Stevens, M. R. Cosby, S. Z. Oener, A. M. Smith, L. J. Enman, K. E. Ayers, C. B. Capuano, J. N. Renner, N. Danilovic, Y. Li, H. Wang, Q. Zhang, S. W. Boettcher, *ACS Catal.* **2019**, *9*, 7–15.
[105] T. Zhang, M. R. Nellist, L. J. Enman, J. Xiang, S. W. Boettcher, *ChemSusChem* **2019**, *12*, 2015–2021.
[106] F. D. Speck, K. E. Dettelbach, R. S. Sherbo, D. A. Salvatore, A. Huang, C. P. Berlinguette, *Chem* **2017**, *2*, 590–597.
[107] D. Tyndall, M. J. Craig, L. Gannon, C. McGuinness, N. McEvoy, A. Roy, M. García-Melchor, M. P. Browne, V. Nicolosi, *J. Mater. Chem. A* **2023**, *11*, 4067–4077.
[108] D. Y. Chung, P. P. Lopes, P. Farinazzo Bergamo Dias Martins, H. He, T. Kawaguchi, P. Zapol, H. You, D. Tripkovic, D. Strmcnik, Y. Zhu, S. Seifert, S. Lee, V. R. Stamenkovic, N. M. Markovic, *Nat. Energy* **2020**, *5*, 222–230.
[109] J. Xiao, A. M. Oliveira, L. Wang, Y. Zhao, T. Wang, J. Wang, B. P. Setzler, Y. Yan, *ACS Catal.* **2021**, *11*, 264–270.

[110] L. Wang, V. A. Saveleva, M. J. Eslamibidgoli, D. Antipin, C. Bouillet, I. Biswas, A. S. Gago, S. S. Hosseiny, P. Gazdzicki, M. H. Eikerling, E. R. Savinova, K. A. Friedrich, *ACS Appl. Energ. Mater.* **2022**, *5*, 2221–2230.
[111] H. Koshikawa, H. Murase, T. Hayashi, K. Nakajima, H. Mashiko, S. Shiraishi, Y. Tsuji, *ACS Catal.* **2020**, *10*, 1886–1893.
[112] Á. Vass, B. Endrődi, G. F. Samu, Á. Balog, A. Kormányos, S. Cherevko, C. Janáky, *ACS Energy Lett.* **2021**, *6*, 3801–3808.
[113] S. Shiva Kumar, V. Himabindu, *Mater. Sci. Energy Technol.* **2019**, *2*, 442–454.
[114] NeoNickel, "Technical Resources Comparison between Titanium Grade 1, Titanium Grade 2, Titanium Grade 3 and Titanium Grade 4," can be found under https://www.neonickel.com/technical-resources/general-technical-resources/comparison-between-titanium-grade-1-titanium-grade-2-titanium-grade-3-and-titanium-grade-4/.
[115] J. Park, H. Oh, T. Ha, Y. Il Lee, K. Min, *Appl. Energy* **2015**, *155*, 866–880.
[116] S. Verma, S. Lu, P. J. A. Kenis, *Nat. Energy* **2019**, *4*, 466–474.
[117] T. Novalin, B. Eriksson, S. K. Proch, U. Bexell, C. Moffatt, J. Westlinder, C. Lagergren, G. Lindbergh, R. Wreland Lindström, *ECS Meeting Abstracts* **2022**, *MA2022–01*, 1457–1457.
[118] Y. C. Tan, W. K. Quek, B. Kim, S. Sugiarto, J. Oh, D. Kai, *ACS Energy Lett.* **2022**, *7*, 2012–2023.
[119] "Fuel Cell System Contaminants Material Screening Data," can be found under https://www.nrel.gov/hydrogen/system-contaminants-data/index.html.
[120] M. Schneider, K. Kremmer, C. Lämmel, K. Sempf, M. Herrmann, *Corros. Sci.* **2014**, *80*, 191–196.
[121] G. S. Frankel, N. Sridhar, *Mater. Today* **2008**, *11*, 38–44.
[122] P. Trogadas, J. Parrondo, V. Ramani, *Electrochem. Solid-State Lett.* **2008**, *11*, B113–B116.
[123] H. Hagihara, H. Uchida, M. Watanabe, *Electrochim. Acta* **2006**, *51*, 3979–3985.
[124] P. Trinke, P. Haug, J. Brauns, B. Bensmann, R. Hanke-Rauschenbach, T. Turek, *J. Electrochem. Soc.* **2018**, *165*, F502–F513.
[125] F. Pantò, S. Siracusano, N. Briguglio, A. S. Aricò, *Appl. Energy* **2020**, *279*, 115809.
[126] A. Stähler, M. Stähler, F. Scheepers, W. Lehnert, M. Carmo, *J. Electrochem. Soc.* **2022**, *169*, 034522.
[127] H. J. Baumgartner, G. C. Hood, J. M. Monger, R. M. Roberts, C. E. Sandborn, *J. Catal.* **1963**, *2*, 405–414.
[128] D. B. Broughton, R. L. Wentworth, *J. Am. Chem. Soc.* **1947**, *69*, 741–744.
[129] C. M. Lousada, A. J. Johansson, T. Brinck, M. Jonsson, *J. Phys. Chem. C* **2012**, *116*, 9533–9543.
[130] J. Kim, H. Lee, E. B. Cho, B. Bae, *ACS Omega* **2021**, *6*, 25551–25561.
[131] S. Yuk, D. W. Lee, K.-Y. Song, S. Choi, D.-H. Lee, G. Doo, J. Hyun, J. Kwen, J. Y. Kim, H.-T. Kim, *J. Power Sources* **2020**, *448*, 227447.
[132] S. M. Stewart, D. Spernjak, R. Borup, A. Datye, F. Garzon, *ECS Electrochem. Lett.* **2014**, *3*, F19–F22.
[133] K. H. Wong, E. Kjeang, *J. Electrochem. Soc.* **2017**, *164*, F1179–F1186.
[134] R. Shiratsuchi, Y. Aikoh, G. Nogami, *J. Electrochem. Soc.* **1993**, *140*, 3479–3482.
[135] B. Jermann, J. Augustynski, *Electrochim. Acta* **1994**, *39*, 1891–1896.
[136] Y. Jännsch, J. J. Leung, M. Hämmerle, E. Magori, K. Wiesner-Fleischer, E. Simon, M. Fleischer, R. Moos, *Electrochem. Commun.* **2020**, *121*, 106861.
[137] J. Lee, Y. Tak, *Electrochim. Acta* **2001**, *46*, 3015–3022.
[138] N. Gupta, M. Gattrell, B. MacDougall, *J. Appl. Electrochem.* **2006**, *36*, 161–172.
[139] Q. Lu, J. Rosen, F. Jiao, *ChemCatChem* **2015**, *7*, 38–47.
[140] J. G. Chen, C. A. Menning, M. B. Zellner, *Surf. Sci. Rep.* **2008**, *63*, 201–254.
[141] F. P. García de Arquer, C.-T. Dinh, A. Ozden, J. Wicks, C. McCallum, A. R. Kirmani, D.-H. Nam, C. Gabardo, A. Seifitokaldani, X. Wang, Y. C. Li, F. Li, J. Edwards, L. J. Richter, S. J. Thorpe, D. Sinton, E. H. Sargent, *Science* **2020**, *367*, 661–666.
[142] I. Grigioni, L. K. Sagar, Y. C. Li, G. Lee, Y. Yan, K. Bertens, R. K. Miao, X. Wang, J. Abed, D. H. Won, F. P. García de Arquer, A. H. Ip, D. Sinton, E. H. Sargent, *ACS Energy Lett.* **2021**, *6*, 79–84.
[143] X. Yan, C. Chen, Y. Wu, S. Liu, Y. Chen, R. Feng, J. Zhang, B. Han, *Chem. Sci.* **2021**, *12*, 6638–6645.
[144] T. Zheng, C. Liu, C. Guo, M. Zhang, X. Li, Q. Jiang, W. Xue, H. Li, A. Li, C. W. Pao, J. Xiao, C. Xia, J. Zeng, *Nat. Nanotechnol.* **2021**, *16*, 1386–1393.
[145] W. Ma, S. Xie, T. Liu, Q. Fan, J. Ye, F. Sun, Z. Jiang, Q. Zhang, J. Cheng, Y. Wang, *Nat. Catal.* **2020**, *3*, 478–487.
[146] B. Endrdi, E. Kecsenovity, A. Samu, T. Halmágyi, S. Rojas-Carbonell, L. Wang, Y. Yan, C. Janáky, *Energy Environ. Sci.* **2020**, *13*, 4098–4105.
[147] B. Endrődi, A. Samu, E. Kecsenovity, T. Halmágyi, D. Sebők, C. Janáky, *Nat. Energy* **2021**, *6*, 439–448.
[148] M. Ma, E. L. Clark, K. T. Therkildsen, S. Dalsgaard, I. Chorkendorff, B. Seger, *Energy Environ. Sci.* **2020**, *13*, 977–985.
[149] H. Haspel, J. Gascon, *ACS Appl. Energ. Mater.* **2021**, *4*, 8506–8516.
[150] T. Haas, R. Krause, R. Weber, M. Demler, G. Schmid, *Nat. Catal.* **2018**, *1*, 32–39.
[151] J. E. Huang, F. Li, A. Ozden, A. S. Rasouli, F. P. G. de Arquer, S. Liu, S. Zhang, M. Luo, X. Wang, Y. Lum, Y. Xu, K. Bertens, R. K. Miao, C. T. Dinh, D. Sinton, E. H. Sargent, *Science* **2021**, *372*, 1074–1078.
[152] X. She, T. Zhang, Z. Li, H. Li, H. Xu, J. Wu, in *AIChE Annual Meeting*, *Conference Proceedings*, American Institute Of Chemical Engineers, **2021**.
[153] J. P. Edwards, Y. Xu, C. M. Gabardo, C. T. Dinh, J. Li, Z. B. Qi, A. Ozden, E. H. Sargent, D. Sinton, *Appl. Energy* **2020**, *261*, 114305.
[154] J. B. Vennekoetter, R. Sengpiel, M. Wessling, *Chem. Eng. J.* **2019**, *364*, 89–101.
[155] A. Ozden, Y. Liu, C. T. Dinh, J. Li, P. Ou, F. P. García De Arquer, E. H. Sargent, D. Sinton, *ACS Appl. Energ. Mater.* **2021**, *4*, 7504–7512.
[156] L. Fan, C. Xia, P. Zhu, Y. Lu, H. Wang, *Nat. Commun.* **2020**, *11*, 3633.
[157] L. Li, A. Ozden, S. Guo, F. P. García de Arquer, C. Wang, M. Zhang, J. Zhang, H. Jiang, W. Wang, H. Dong, D. Sinton, E. H. Sargent, M. Zhong, *Nat. Commun.* **2021**, *12*, 5223.
[158] X. Wang, Z. Wang, F. P. García de Arquer, C. T. Dinh, A. Ozden, Y. C. Li, D. H. Nam, J. Li, Y. S. Liu, J. Wicks, Z. Chen, M. Chi, B. Chen, Y. Wang, J. Tam, J. Y. Howe, A. Proppe, P. Todorović, F. Li, T. T. Zhuang, C. M. Gabardo, A. R. Kirmani, C. McCallum, S. F. Hung, Y. Lum, M. Luo, Y. Min, A. Xu, C. P. O'Brien, B. Stephen, B. Sun, A. H. Ip, L. J. Richter, S. O. Kelley, D. Sinton, E. H. Sargent, *Nat. Energy* **2020**, *5*, 478–486.
[159] F. Li, A. Thevenon, A. Rosas-Hernández, Z. Wang, Y. Li, C. M. Gabardo, A. Ozden, C. T. Dinh, J. Li, Y. Wang, J. P. Edwards, Y. Xu, C. McCallum, L. Tao, Z. Q. Liang, M. Luo, X. Wang, H. Li, C. P. O'Brien, C. S. Tan, D. H. Nam, R. Quintero-Bermudez, T. T. Zhuang, Y. C. Li, Z. Han, R. D.

Britt, D. Sinton, T. Agapie, J. C. Peters, E. H. Sargent, *Nature* **2020**, *577*, 509–513.
[160] F. Li, Y. C. Li, Z. Wang, J. Li, D. H. Nam, Y. Lum, M. Luo, X. Wang, A. Ozden, S. F. Hung, B. Chen, Y. Wang, J. Wicks, Y. Xu, Y. Li, C. M. Gabardo, C. T. Dinh, Y. Wang, T. T. Zhuang, D. Sinton, E. H. Sargent, *Nat. Catal.* **2020**, *3*, 75–82.
[161] Y. Wang, Z. Wang, C. T. Dinh, J. Li, A. Ozden, M. Golam Kibria, A. Seifitokaldani, C. S. Tan, C. M. Gabardo, M. Luo, H. Zhou, F. Li, Y. Lum, C. McCallum, Y. Xu, M. Liu, A. Proppe, A. Johnston, P. Todorovic, T. T. Zhuang, D. Sinton, S. O. Kelley, E. H. Sargent, *Nat. Catal.* **2020**, *3*, 98–106.
[162] Q. Wan, Q. He, Y. Zhang, L. Zhang, J. Li, J. Hou, X. Zhuang, C. Ke, J. Zhang, *Electrochim. Acta* **2021**, *392*, 139023.
[163] R. Xia, J. J. Lv, X. Ma, F. Jiao, *J. Catal.* **2021**, *398*, 185–191.
[164] S. S. Bhargava, E. R. Cofell, P. Chumble, D. Azmoodeh, S. Someshwar, P. J. A. Kenis, *Electrochim. Acta* **2021**, *394*, 139055.
[165] T. Zhang, S. Verma, S. Kim, T. T. Fister, P. J. A. Kenis, A. A. Gewirth, *J. Electroanal. Chem.* **2020**, *875*, 113862.
[166] W. H. Lee, Y.-J. Ko, Y. Choi, S. Y. Lee, C. H. Choi, Y. J. Hwang, B. K. Min, P. Strasser, H.-S. Oh, *Nano Energy* **2020**, *76*, 105030.
[167] A. Del Castillo, M. Alvarez-Guerra, J. Solla-Gullón, A. Sáez, V. Montiel, A. Irabien, *J. CO2 Util.* **2017**, *18*, 222–228.
[168] H. Yang, J. J. Kaczur, S. D. Sajjad, R. I. Masel, *J. CO2 Util.* **2017**, *20*, 208–217.
[169] C. M. Gabardo, C. P. O'Brien, J. P. Edwards, C. McCallum, Y. Xu, C. T. Dinh, J. Li, E. H. Sargent, D. Sinton, *Joule* **2019**, *3*, 2777–2791.
[170] S. E. Weitzner, S. A. Akhade, A. R. Kashi, Z. Qi, A. K. Buckley, Z. Huo, S. Ma, M. Biener, B. C. Wood, K. P. Kuhl, J. B. Varley, J. Biener, *J. Chem. Phys.* **2021**, *155*, 114702.
[171] Y. Wang, H. Shen, K. J. T. Livi, D. Raciti, H. Zong, J. Gregg, M. Onadeko, Y. Wan, A. Watson, C. Wang, *Nano Lett.* **2019**, *19*, 8461–8468.
[172] U. O. Nwabara, A. D. Hernandez, D. A. Henckel, X. Chen, E. R. Cofell, M. P. De-Heer, S. Verma, A. A. Gewirth, P. J. A. Kenis, *ACS Appl. Energ. Mater.* **2021**, *4*, 5175–5186.
[173] E. R. Cofell, U. O. Nwabara, S. S. Bhargava, D. E. Henckel, P. J. A. Kenis, *ACS Appl. Mater. Interfaces* **2021**, *13*, 15132–15142.
[174] G. O. Larrazábal, P. Strøm-Hansen, J. P. Heli, K. Zeiter, K. T. Therkildsen, I. Chorkendorff, B. Seger, *ACS Appl. Mater. Interfaces* **2019**, *11*, 41281–41288.
[175] A. Ozden, F. Li, F. P. García De Arquer, A. Rosas-Hernández, A. Thevenon, Y. Wang, S. F. Hung, X. Wang, B. Chen, J. Li, J. Wicks, M. Luo, Z. Wang, T. Agapie, J. C. Peters, E. H. Sargent, D. Sinton, *ACS Energy Lett.* **2020**, *5*, 2811–2818.
[176] S. S. Bhargava, D. Azmoodeh, X. Chen, E. R. Cofell, A. M. Esposito, S. Verma, A. A. Gewirth, P. J. A. Kenis, *ACS Energy Lett.* **2021**, *6*, 2427–2433.
[177] C. P. O'Brien, R. K. Miao, S. Liu, Y. Xu, G. Lee, A. Robb, J. E. Huang, K. Xie, K. Bertens, C. M. Gabardo, J. P. Edwards, C. T. Dinh, E. H. Sargent, D. Sinton, *ACS Energy Lett.* **2021**, *6*, 2952–2959.
[178] D. Kim, W. Choi, H. W. Lee, S. Y. Lee, Y. Choi, D. K. Lee, W. Kim, J. Na, U. Lee, Y. J. Hwang, D. H. Won, *ACS Energy Lett.* **2021**, *6*, 3488–3495.
[179] S. Verma, Y. Hamasaki, C. Kim, W. Huang, S. Lu, H. R. M. Jhong, A. A. Gewirth, T. Fujigaya, N. Nakashima, P. J. A. Kenis, *ACS Energy Lett.* **2018**, *3*, 193–198.
[180] B. Endrődi, E. Kecsenovity, A. Samu, F. Darvas, R. V. Jones, V. Török, A. Danyi, C. Janáky, *ACS Energy Lett.* **2019**, *4*, 1770–1777.
[181] J. Li, J. Jiao, H. Zhang, P. Zhu, H. Ma, C. Chen, H. Xiao, Q. Lu, *ACS Sustainable Chem. Eng.* **2020**, *8*, 4975–4982.
[182] A. N. Kuhn, H. Zhao, U. O. Nwabara, X. Lu, M. Liu, Y. Pan, W. Zhu, P. J. A. Kenis, H. Yang, *Adv. Funct. Mater.* **2021**, *31*, 2101668.
[183] J. Lv, M. Jouny, W. Luc, W. Zhu, J. Zhu, F. Jiao, *Adv. Mater.* **2018**, *30*, 1803111.
[184] F. Gao, S. Hu, X. Zhang, Y. Zheng, H. Wang, Z. Niu, P. Yang, R. Bao, T. Ma, Z. Dang, Y. Guan, X. Zheng, X. Zheng, J. Zhu, M. Gao, S. Yu, *Angew. Chem. Int. Ed.* **2020**, *59*, 8706–8712.
[185] T. Möller, F. Scholten, T. N. Thanh, I. Sinev, J. Timoshenko, X. Wang, Z. Jovanov, M. Gliech, B. Roldan Cuenya, A. S. Varela, P. Strasser, *Angew. Chem. Int. Ed.* **2020**, *59*, 17974–17983.
[186] H. Li, T. Liu, P. Wei, L. Lin, D. Gao, G. Wang, X. Bao, *Angew. Chem. Int. Ed.* **2021**, *60*, 14329–14333.
[187] T. Möller, W. Ju, A. Bagger, X. Wang, F. Luo, T. Ngo Thanh, A. S. Varela, J. Rossmeisl, P. Strasser, *Energy Environ. Sci.* **2019**, *12*, 640–647.
[188] Z. Yin, H. Peng, X. Wei, H. Zhou, J. Gong, M. Huai, L. Xiao, G. Wang, J. Lu, L. Zhuang, *Energy Environ. Sci.* **2019**, *12*, 2455–2462.
[189] H. Y. Jeong, M. Balamurugan, V. S. K. Choutipalli, E. S. Jeong, V. Subramanian, U. Sim, K. T. Nam, *J. Mater. Chem. A* **2019**, *7*, 10651–10661.
[190] J. Wang, J. Zou, X. Hu, S. Ning, X. Wang, X. Kang, S. Chen, *J. Mater. Chem. A* **2019**, *7*, 27514–27521.
[191] S. S. Bhargava, F. Proietto, D. Azmoodeh, E. R. Cofell, D. A. Henckel, S. Verma, C. J. Brooks, A. A. Gewirth, P. J. A. Kenis, *ChemElectroChem* **2020**, *7*, 2001–2011.
[192] R. Krause, D. Reinisch, C. Reller, H. Eckert, D. Hartmann, D. Taroata, K. Wiesner-Fleischer, A. Bulan, A. Lueken, G. Schmid, *Chem. Ing. Tech.* **2020**, *92*, 53–61.
[193] N. Martić, C. Reller, C. Macauley, M. Löffler, A. M. Reichert, T. Reichbauer, K. M. Vetter, B. Schmid, D. McLaughlin, P. Leidinger, D. Reinisch, C. Vogl, K. J. J. Mayrhofer, I. Katsounaros, G. Schmid, *Energy Environ. Sci.* **2020**, *13*, 2993–3006.
[194] M. Li, M. N. Idros, Y. Wu, S. Garg, S. Gao, R. Lin, H. Rabiee, Z. Li, L. Ge, T. E. Rufford, Z. Zhu, L. Li, G. Wang, *React. Chem. Eng.* **2021**, *6*, 345–352.
[195] J. J. Kaczur, H. Yang, Z. Liu, S. D. Sajjad, R. I. Masel, *Front. Chem.* **2018**, *6*, 263.
[196] T. T. H. Hoang, S. Verma, S. Ma, T. T. Fister, J. Timoshenko, A. I. Frenkel, P. J. A. Kenis, A. A. Gewirth, *J. Am. Chem. Soc.* **2018**, *140*, 5791–5797.
[197] X. Wang, K. Klingan, M. Klingenhof, T. Möller, J. Ferreira de Araújo, I. Martens, A. Bagger, S. Jiang, J. Rossmeisl, H. Dau, P. Strasser, *Nat. Commun.* **2021**, *12*, 794.
[198] J. Li, A. Ozden, M. Wan, Y. Hu, F. Li, Y. Wang, R. R. Zamani, D. Ren, Z. Wang, Y. Xu, D.-H. Nam, J. Wicks, B. Chen, X. Wang, M. Luo, M. Graetzel, F. Che, E. H. Sargent, D. Sinton, *Nat. Commun.* **2021**, *12*, 2808.
[199] Y. Xu, F. Li, A. Xu, J. P. Edwards, S.-F. Hung, C. M. Gabardo, C. P. O'Brien, S. Liu, X. Wang, Y. Li, J. Wicks, R. K. Miao, Y. Liu, J. Li, J. E. Huang, J. Abed, Y. Wang, E. H. Sargent, D. Sinton, *Nat. Commun.* **2021**, *12*, 2932.
[200] M. Esmaeilirad, A. Baskin, A. Kondori, A. Sanz-Matias, J. Qian, B. Song, M. Tamadoni Saray, K. Kucuk, A. R. Belmonte, P. N. M. Delgado, J. Park, R. Azari, C. U. Segre, R. Shahbazian-Yassar, D. Prendergast, M. Asadi, *Nat. Commun.* **2021**, *12*, 5067.
[201] X. Chen, J. Chen, N. M. Alghoraibi, D. A. Henckel, R. Zhang, U. O. Nwabara, K. E. Madsen, P. J. A. Kenis, S. C. Zimmerman, A. A. Gewirth, *Nat. Catal.* **2021**, *4*, 20–27.
[202] W. R. Leow, Y. Lum, A. Ozden, Y. Wang, D. H. Nam, B. Chen, J. Wicks, T. T. Zhuang, F. Li, D. Sinton, E. H. Sargent, *Science* **2020**, *368*, 1228–1233.

[203] Y. Chen, A. Vise, W. E. Klein, F. C. Cetinbas, D. J. Myers, W. A. Smith, W. A. Smith, W. A. Smith, T. G. Deutsch, K. C. Neyerlin, *ACS Energy Lett.* **2020**, *5*, 1825–1833.
[204] E. W. Lees, M. Goldman, A. G. Fink, D. J. Dvorak, D. A. Salvatore, Z. Zhang, N. W. X. Loo, C. P. Berlinguette, *ACS Energy Lett.* **2020**, *5*, 2165–2173.
[205] D. A. Salvatore, D. M. Weekes, J. He, K. E. Dettelbach, Y. C. Li, T. E. Mallouk, C. P. Berlinguette, *ACS Energy Lett.* **2018**, *3*, 149–154.
[206] R. Wang, H. Haspel, A. Pustovarenko, A. Dikhtiarenko, A. Russkikh, G. Shterk, D. Osadchii, S. Ould-Chikh, M. Ma, W. A. Smith, K. Takanabe, F. Kapteijn, J. Gascon, *ACS Energy Lett.* **2019**, *4*, 2024–2031.
[207] A. Sedighian Rasouli, X. Wang, J. Wicks, G. Lee, T. Peng, F. Li, C. McCallum, C.-T. Dinh, A. H. Ip, D. Sinton, E. H. Sargent, *ACS Sustainable Chem. Eng.* **2020**, *8*, 14668–14673.
[208] M. G. Kibria, C.-T. Dinh, A. Seifitokaldani, P. De Luna, T. Burdyny, R. Quintero-Bermudez, M. B. Ross, O. S. Bushuyev, F. P. García de Arquer, P. Yang, D. Sinton, E. H. Sargent, *Adv. Mater.* **2018**, *30*, 1804867.
[209] H. Xie, T. Zhang, R. Xie, Z. Hou, X. Ji, Y. Pang, S. Chen, M. Titirici, H. Weng, G. Chai, *Adv. Mater.* **2021**, *33*, 2008373.
[210] L. Xiong, X. Zhang, L. Chen, Z. Deng, S. Han, Y. Chen, J. Zhong, H. Sun, Y. Lian, B. Yang, X. Yuan, H. Yu, Y. Liu, X. Yang, J. Guo, M. H. Rümmeli, Y. Jiao, Y. Peng, *Adv. Mater.* **2021**, *33*, 2101741.
[211] J. Yang, X. Wang, Y. Qu, X. Wang, H. Huo, Q. Fan, J. Wang, L. M. Yang, Y. Wu, *Adv. Energy Mater.* **2020**, *10*, 2001709.
[212] Q. Fan, X. Zhang, X. Ge, L. Bai, D. He, Y. Qu, C. Kong, J. Bi, D. Ding, Y. Cao, X. Duan, J. Wang, J. Yang, Y. Wu, *Adv. Energy Mater.* **2021**, *11*, 2101424–2101434.
[213] C. Chen, X. Yan, S. Liu, Y. Wu, Q. Wan, X. Sun, Q. Zhu, H. Liu, J. Ma, L. Zheng, H. Wu, B. Han, *Angew. Chem. Int. Ed.* **2020**, *59*, 16459–16464.
[214] C. M. Gabardo, A. Seifitokaldani, J. P. Edwards, C.-T. Dinh, T. Burdyny, M. G. Kibria, C. P. O'Brien, E. H. Sargent, D. Sinton, *Energy Environ. Sci.* **2018**, *11*, 2531–2539.
[215] E. W. Lees, B. A. W. Mowbray, D. A. Salvatore, G. L. Simpson, D. J. Dvorak, S. Ren, J. Chau, K. L. Milton, C. P. Berlinguette, *J. Mater. Chem. A* **2020**, *8*, 19493–19501.
[216] C. Chen, X. Yan, Y. Wu, S. Liu, X. Sun, Q. Zhu, R. Feng, T. Wu, Q. Qian, H. Liu, L. Zheng, J. Zhang, B. Han, *Chem. Sci.* **2021**, *12*, 5938–5943.
[217] P.-P. Yang, X.-L. Zhang, F.-Y. Gao, Y.-R. Zheng, Z.-Z. Niu, X. Yu, R. Liu, Z.-Z. Wu, S. Qin, L.-P. Chi, Y. Duan, T. Ma, X.-S. Zheng, J.-F. Zhu, H.-J. Wang, M.-R. Gao, S.-H. Yu, *J. Am. Chem. Soc.* **2020**, *142*, 6400–6408.
[218] D. Niu, C. Wei, Z. Lu, Y. Fang, B. Liu, D. Sun, X. Hao, H. Pan, G. Wang, *Molecules* **2021**, *26*, 2175.
[219] M. Luo, Z. Wang, Y. C. Li, J. Li, F. Li, Y. Lum, D. H. Nam, B. Chen, J. Wicks, A. Xu, T. Zhuang, W. R. Leow, X. Wang, C. T. Dinh, Y. Wang, Y. Wang, D. Sinton, E. H. Sargent, *Nat. Commun.* **2019**, *10*, 5814.
[220] Y. Li, A. Xu, Y. Lum, X. Wang, S.-F. Hung, B. Chen, Z. Wang, Y. Xu, F. Li, J. Abed, J. E. Huang, A. S. Rasouli, J. Wicks, L. K. Sagar, T. Peng, A. H. Ip, D. Sinton, H. Jiang, C. Li, E. H. Sargent, *Nat. Commun.* **2020**, *11*, 6190.
[221] X. Wang, P. Ou, J. Wicks, Y. Xie, Y. Wang, J. Li, J. Tam, D. Ren, J. Y. Howe, Z. Wang, A. Ozden, Y. Z. Finfrock, Y. Xu, Y. Li, A. S. Rasouli, K. Bertens, A. H. Ip, M. Graetzel, D. Sinton, E. H. Sargent, *Nat. Commun.* **2021**, *12*, 3387.
[222] S. Ren, D. Joulié, D. Salvatore, K. Torbensen, M. Wang, M. Robert, C. P. Berlinguette, *Science* **2019**, *365*, 367–369.
[223] T. Burdyny, W. A. Smith, *Energy Environ. Sci.* **2019**, *12*, 1442–1453.
[224] M. Abdinejad, C. Dao, X. an Zhang, H. B. Kraatz, *J. Energy Chem.* **2021**, *58*, 162–169.
[225] D. Kim, S. Yu, F. Zheng, I. Roh, Y. Li, S. Louisia, Z. Qi, G. A. Somorjai, H. Frei, L.-W. Wang, P. Yang, *Nat. Energy* **2020**, *5*, 1032–1042.
[226] M. Zhong, K. Tran, Y. Min, C. Wang, Z. Wang, C. T. Dinh, P. De Luna, Z. Yu, A. S. Rasouli, P. Brodersen, S. Sun, O. Voznyy, C. S. Tan, M. Askerka, F. Che, M. Liu, A. Seifitokaldani, Y. Pang, S. C. Lo, A. Ip, Z. Ulissi, E. H. Sargent, *Nature* **2020**, *581*, 178–183.
[227] S. C. Perry, S. M. Gateman, R. Malpass-Evans, N. McKeown, M. Wegener, P. Nazarovs, J. Mauzeroll, L. Wang, C. Ponce de León, *Chemosphere* **2020**, *248*, 125993.
[228] H. Rabiee, L. Ge, X. Zhang, S. Hu, M. Li, S. Smart, Z. Zhu, H. Wang, Z. Yuan, *Appl. Catal. B* **2021**, *298*, 120538.
[229] B. De Mot, J. Hereijgers, M. Duarte, T. Breugelmans, *Chem. Eng. J.* **2019**, *378*, 122224.
[230] M. Duarte, N. Daems, J. Hereijgers, D. Arenas-Esteban, S. Bals, T. Breugelmans, *J. CO2 Util.* **2021**, *50*, 101583.
[231] C. Chen, Y. Li, S. Yu, S. Louisia, J. Jin, M. Li, M. B. Ross, P. Yang, *Joule* **2020**, *4*, 1688–1699.
[232] M. de Jesus Gálvez-Vázquez, P. Moreno-García, H. Xu, Y. Hou, H. Hu, I. Z. Montiel, A. V. Rudnev, S. Alinejad, V. Grozovski, B. J. Wiley, M. Arenz, P. Broekmann, *ACS Catal.* **2020**, *10*, 13096–13108.
[233] H. Xiang, H. A. Miller, M. Bellini, H. Christensen, K. Scott, S. Rasul, E. H. Yu, *Sustain. Energy Fuels* **2020**, *4*, 277–284.
[234] M. Duarte, B. De Mot, J. Hereijgers, T. Breugelmans, *ChemElectroChem* **2019**, *6*, 5596–5602.
[235] J. C. Lee, J. Y. Kim, W. H. Joo, D. Hong, S. H. Oh, B. Kim, G. Do Lee, M. Kim, J. Oh, Y. C. Joo, *J. Mater. Chem. A* **2020**, *8*, 11632–11641.
[236] H. S. Jeon, J. Timoshenko, C. Rettenmaier, A. Herzog, A. Yoon, S. W. Chee, S. Oener, U. Hejral, F. T. Haase, B. Roldan Cuenya, *J. Am. Chem. Soc.* **2021**, *143*, 7578–7587.
[237] H. Yang, Q. Lin, C. Zhang, X. Yu, Z. Cheng, G. Li, Q. Hu, X. Ren, Q. Zhang, J. Liu, C. He, *Nat. Commun.* **2020**, *11*, 1–8.
[238] R. Shi, J. Guo, X. Zhang, G. I. N. Waterhouse, Z. Han, Y. Zhao, L. Shang, C. Zhou, L. Jiang, T. Zhang, *Nat. Commun.* **2020**, *11*, 3028.
[239] X. Wu, Y. Guo, Z. Sun, F. Xie, D. Guan, J. Dai, F. Yu, Z. Hu, Y. C. Huang, C. W. Pao, J. L. Chen, W. Zhou, Z. Shao, *Nat. Commun.* **2021**, *12*, 1–11.
[240] S. Li, Y. Ma, T. Zhao, J. Li, X. Kang, W. Guo, Y. Wen, L. Wang, Y. Wang, R. Lin, T. Li, H. Tan, H. Peng, B. Zhang, *ChemistryOpen* **2021**, *10*, 639–644.
[241] Y. C. Tan, K. B. Lee, H. Song, J. Oh, *Joule* **2020**, *4*, 1104–1120.
[242] D. Choukroun, L. Pacquets, C. Li, S. Hoekx, S. Arnouts, K. Baert, T. Hauffman, S. Bals, T. Breugelmans, *ACS Nano* **2021**, *15*, 14858–14872.
[243] S. A. Abbas, J. T. Song, Y. C. Tan, K. M. Nam, J. Oh, K. D. Jung, *ACS Appl. Energ. Mater.* **2020**, *3*, 8739–8745.
[244] A. Peugeot, C. E. Creissen, M. W. Schreiber, M. Fontecave, *ChemElectroChem* **2021**, *8*, 2726–2736.
[245] X. Zhang, Y. Wang, M. Gu, M. Wang, Z. Zhang, W. Pan, Z. Jiang, H. Zheng, M. Lucero, H. Wang, G. E. Sterbinsky, Q. Ma, Y. G. Wang, Z. Feng, J. Li, H. Dai, Y. Liang, *Nat. Energy* **2020**, *5*, 684–692.
[246] H. Xiang, S. Rasul, B. Hou, J. Portoles, P. Cumpson, E. H. Yu, *ACS Appl. Mater. Interfaces* **2020**, *12*, 601–608.
[247] J. Wicks, M. L. Jue, V. A. Beck, J. S. Oakdale, N. A. Dudukovic, A. L. Clemens, S. Liang, M. E. Ellis, G. Lee, S. E. Baker, E. B. Duoss, E. H. Sargent, *Adv. Mater.* **2021**, *33*, 2003855.
[248] C. Cao, D. Ma, J. Gu, X. Xie, G. Zeng, X. Li, S. Han, Q. Zhu, X. Wu, Q. Xu, *Angew. Chem. Int. Ed.* **2020**, *59*, 15014–15020.
[249] L. Cheng, Y. Wang, Y. Li, Y. Shen, Y. Zhen, Z. Xing, L. Lin, A. Chen, Y. Zhu, C. Li, *ChemCatChem* **2021**, *13*, 1161–1164.

[250] J. Lee, J. Lim, C.-W. Roh, H. S. Whang, H. Lee, *J. CO2 Util.* **2019**, *31*, 244–250.
[251] W. Lee, Y. E. Kim, M. H. Youn, S. K. Jeong, K. T. Park, *Angew. Chem. Int. Ed.* **2018**, *57*, 6883–6887.
[252] C. Xia, P. Zhu, Q. Jiang, Y. Pan, W. Liang, E. Stavitski, H. N. Alshareef, H. Wang, *Nat. Energy* **2019**, *4*, 776–785.
[253] S. Verma, X. Lu, S. Ma, R. I. Masel, P. J. A. Kenis, *Phys. Chem. Chem. Phys.* **2016**, *18*, 7075–7084.
[254] O. Romiluyi, N. Danilovic, A. T. Bell, A. Z. Weber, *Electrochem. Sci. Adv.* **2023**, *3*, e2100186.
[255] Z. Liu, H. Yang, R. Kutz, R. I. Masel, *J. Electrochem. Soc.* **2018**, *165*, J3371–J3377.
[256] W. Choi, Y. Choi, E. Choi, H. Yun, W. Jung, W. H. Lee, H.-S. Oh, D. H. Won, J. Na, Y. J. Hwang, *J. Mater. Chem. A* **2022**, *10*, 10363–10372.
[257] N. R. de Tacconi, W. Chanmanee, B. H. Dennis, K. Rajeshwar, *J. Mater. Res.* **2017**, *32*, 1727–1734.
[258] C.-T. Dinh, F. P. García de Arquer, D. Sinton, E. H. Sargent, *ACS Energy Lett.* **2018**, *3*, 2835–2840.

Manuscript received: May 9, 2023
Accepted manuscript online: July 19, 2023
Version of record online: November 6, 2023